Frauenklinik und Poliklinik der Technischen Universität München,
Klinikum rechts der Isar

High-affinity urokinase-derived cyclic peptides inhibiting urokinase/urokinase receptor-interaction: effects on tumor growth and spread

Sumito Sato

Vollständiger Abdruck der von der Fakultät für Medizin der Technischen Universität München zur Erlangung des akademischen Grades eines

Doktors der Medizin (Dr. med.)

genehmigten Dissertation.

Vorsitzender: Univ.-Prof. Dr. D. Neumeier

Prüfer der Dissertation:

1. Priv.-Doz. Dr. V. Magdolen

2. Univ.-Prof. Dr. M. Schmitt

Die Dissertation wurde am 16.06.2008 bei der Technischen Universität München eingereicht und durch die Fakultät für Medizin am18.03.2009 angenommen.

1. Summary

2. Introduction
- 2.1 The urokinase-type plasminogen activator system in tumor invasion and metastasis
- 2.2 Competitive antagonists of uPA/uPAR-interaction derived from the uPAR binding site of uPA

3. Materials and Methods
- 3.1 Reagents
- 3.2 Cell lines
- 3.3 uPA, uPAR and PAI-1 ELISA
- 3.4 Proliferation assay
- 3.5 Invasion assay
- 3.6 Adhesion assay
- 3.7 Animal model
- 3.8 Statistical analyses

4. Results
- 4.1 Determination of uPA, PAI-1 and uPAR by ELISA
- 4.2 Characterization of proliferation of OvMz-6 cell lines
- 4.3 Invasive capacity of OvMz-6 cells
- 4.4 Biological activity of OvMz-6 in cell adhesion assay
- 4.5 Effect of synthetic cyclic competitive uPA-derived peptide WX-360 and WX-360-Nle in vivo

5. Discussion

6. Acknowledgements

7. References

8. Curriculum vitae

1. Summary

Tumor cell invasion and metastasis depend on the coordinated and temporal expression of proteolytic enzymes to degrade the surrounding extracellular matrix. The tumor cell-associated urokinase-type plasminogen activator system, consisting of the serine protease plasmin, urokinase-type plasminogen activator (uPA), its specific receptor uPAR (CD87), and the two inhibitors PAI-1 and PAI-2, plays an important role in these pericellular processes. Especially, association of the proteolytic activity of uPA with the cell surface via interaction with uPAR significantly increases the invasive capacity of tumor cells, uPA/uPAR system becomes an attractive novel target for anti-metastatic therapy. uPA binds with high affinity to its specific cell surface receptor, uPAR *via* a binding site within the N-terminal region of the molecule.

Previously, the minimal binding region spanning amino acids 19-31 of uPA was determined. A synthetic cyclic uPA-derived peptide, cyclo^{19,31}uPA$_{19-31}$ was designed, serving as a lead structure for the development of two small uPA-derived competitive peptide antagonists to interfere with uPA/uPAR-interaction based on the uPAR binding site in uPA: WX-360 (cyclo^{21,29} [D-Cys21]-uPA$_{21-30}$ [S21C;H29C]) and its norleucine (Nle) derivative WX-360-Nle (cyclo^{21,29}[D-Cys21] -uPA$_{21-30}$ [S21C;K23Nle;H29C]). These peptides display an only five to ten-fold lower affinity to uPAR as compared to the naturally occurring uPAR-ligand uPA.

In this study, we investigated the characteristics of OvMz-6 human ovary cancer cells, which typically induce a large primary and intraperitoneal tumor metastases, and WX-360 and WX-360-Nle were tested in nude mice for their potency to inhibit tumor growth and intraperitoneal spread of *lacZ* tagged OvMz-6. Intraperitoneal administration of cyclic peptide (20 mg peptide/kg; 1U daily for 37 days) into tumor-bearing nude mice resulted in a significant reduction of tumor weight and spread within the peritoneum as compared to the untreated control group. This is the first report demonstrating effective reduction of tumor growth and spread of human ovarian

cancer cells *in vivo* by small synthetic uPA-derived cyclic peptides competitively interfering with uPA/uPAR-interaction. Thus, both WX-360 and WX-360-Nle are promising novel compounds to reduce dissemination of human ovarian carcinoma.

2. Introduction

2.1 The urokinase-type plasminogen activator system in tumor invasion and metastasis

Invasion and metastasis of solid tumors are complex multi-step processes. The invasive behavior of malignant tumor cells and their ability to form distant metastases are facilitated by different cell-associated proteolytic systems. In the host, the extracellular matrix provides a structural barrier for the tumor cells, and malignant cells are able to degrade proteins of the extracellular matrix and basement membrane, leading to local invasion of the tissue and metastasis. Proteolysis is involved in all the steps of the metastatic cascade, namely detachment of tumor cells from the primary tumor site, intravasation, dissemination through the blood circulation or the lymphatic system, extravasation, and formation of metastases at distant sites (Schmitt *et al*., 1997). Various proteolytic systems, including the urokinase-type plasminogen activator (uPA) system, matrix metalloproteinases (MMPs), and cysteine proteases (cathepsin B, L), which partly interact and cooperate, contribute to the net proteolytic activity at the tumor-host interface (Fig. 1) (Andreasen *et al*., 2000, Chapman *et al*., 1997, Noel *et al*., 1997, Schmitt *et al*., 2000, Yan *et al*., 1998). Not only the tumor cells but also stromal cells present within the surrounding tissue or extracellular matrix synthesize components of the different proteolytic systems, thus contributing to proteolysis on the surface of tumor cells (Dublin *et al*., 2000).

The urokinase-type plasminogen activator (uPA) system plays a pivotal role in this degradation process, with components like the serine protease plasmin, its activator urokinase-type plasminogen activator (uPA), the cell surface-associated uPA receptor uPAR (CD87), and the two inhibitors, plasminogen activator inhibitor type 1 (PAI-1) and type 2 (PAI-2) (Fig. 2). For numerous types of solid malignant tumors, a strong clinical value of the plasminogen activation system in predicting disease recurrence and survival in cancer patients has been demonstrated. Patients with low levels of both

uPA and PAI-1 in their primary tumors have a much better prognosis than patients with elevated levels of both factors, emphasizing their fundamental role in tumor invasion and metastasis (Duffy *et al*., 2002, Harbeck *et al*., 2002, Jänicke *et al*., 2001, Look *et al*., 2002, Schmitt *et al*., 2000).

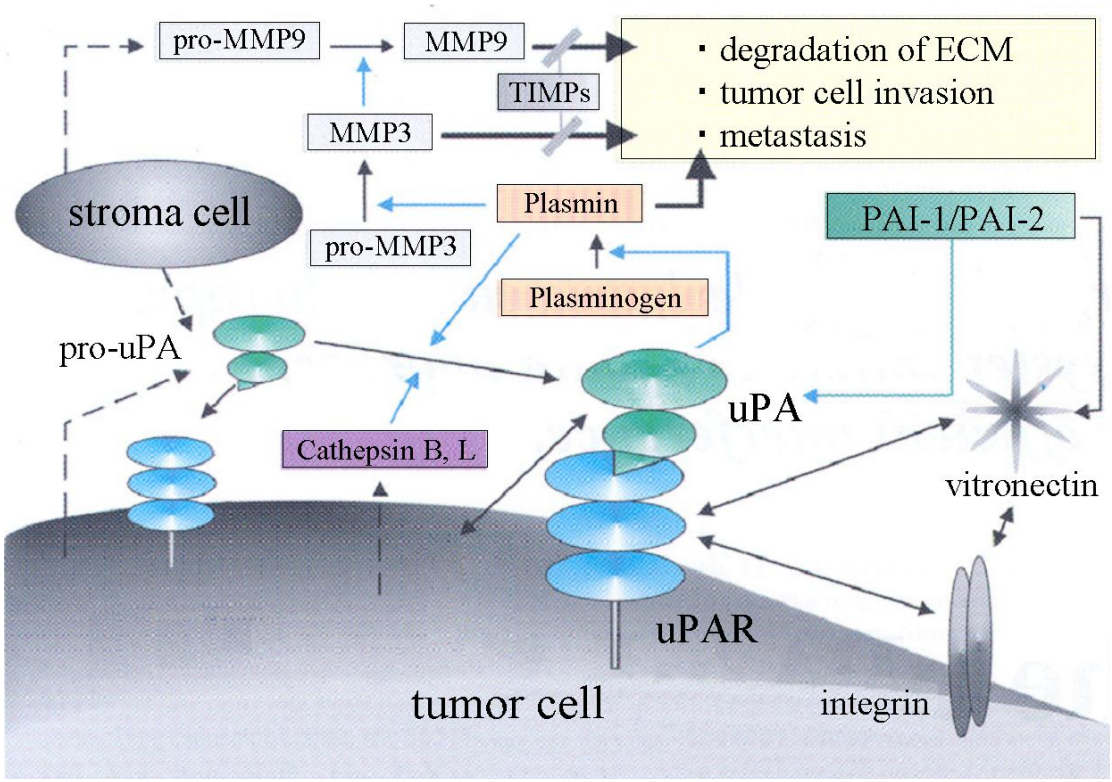

Figure 1. The urokinase-type plasminogen activator system: (pro)-uPA, uPAR and plasmin(ogen) interplay with other extracellular components [e.g., MMPs (-3, -9), cathepsins (B, L), vitronectin and integrins] which leads to degradation of the extracellular matrix and basement membranes, thereby supporting tumor cell invasion and metastasis.

The serine protease uPA (M_r: approximately 55,000), which plays a central role in the conversion of plasminogen to plasmin, is secreted by various normal and cancer cells as a single-chain polypeptide (pro-uPA). pro-uPA consists of 411 amino acids (aa), and several proteases, e.g. plasmin, plasma or glandular tissue kallikrein, and cathepsin B or L (Dano *et al*., 1985), are able to convert pro-uPA by limited proteolysis into the enzymatically active serine protease, HMW-uPA ("high-molecular-weight-uPA"), by cleavage of the peptide bond between Lys^{158} and Ile^{159}. The A-chain of uPA (aa 1-158) and the B-chain (aa 159-411) are covalently connected via a disulfide bridge between Cys^{148} and Cys^{279}. The B-chain harbors the active site of the serine protease with its catalytic triad His^{204}, Asp^{255}, and Ser^{356} (Fig. 3). By further proteolytic action on HMW-uPA, an amino-terminal fragment (ATF; aa 1-135) is released yielding the "low-molecular-weight" form of uPA (LMW-uPA). Both HMW- and LMW-uPA display very similar enzymatic activities towards the substrate plasminogen. ATF consists of two different domains (Fig. 3), the so-called growth factor-like domain (GFD; aa 1-49) and the kringle domain (aa 50-135) which displays structural homology to the kringle domains of e.g. prothrombin, tPA, and plasmin.

The cell surface-associated uPA receptor uPAR (CD87) is a cysteine-rich, heavily N-glycosylated protein of M_r: 45 - 60,000. It is translated into a 313 amino acid polypeptide with a 21 amino acid signal peptide. It consists of three homologous repeats: domains I, II, and III, as numbered from the N terminus (Fig. 4) (Fowler *et al*., 1998, Mondino *et al*., 1999, Ploug *et al*., 2002). uPAR lacks a transmembrane sequences, and is associated with cell membranes by a glycosyl phosphatidyl inositol (GPI) anchor (Ploug *et al.*, 1991). Soluble uPAR variants without a GPI anchor have also been identified in the conditioned medium from various cell lines and in body fluids from cancer patients, and may arise by differential splicing, by proteolysis, or by phospholipase cleavage of the GPI anchor (Brunner *et al.,* 1999, Pedersen *et al.,* 1993,). Required structural determinants for binding of uPA are located within the N-terminal domain I of uPAR. Within this domain residues Arg^{53}, Leu^{55}, Tyr^{57}, and Leu^{66}, respectively, were identified to be essential for the uPA/uPAR interaction, as shown by

a systematic Ala scan (Gårdsvoll *et al*., 1999). However, as shown by several different approaches, the intact three-domain uPAR molecule is required for high-affinity interaction with uPA (Gardsvoll *et al.,* 2006, Llinas *et al.,* 2005, Ploug *et al*., 1998, Ploug *et al*., 2002)

Binding of uPA to its specific high-affinity receptor uPAR (CD87; Kd ~ 1 nM) is mediated by the N-terminally located GFD of uPA, whereas pro-uPA has an activity about 250-fold less than that two-chain uPA (Petersen *et al*., 1988). pro-uPA is activated into uPA either in solution or when bound to uPAR at the cell surface, the latter activation occurs much faster. Furthermore, active uPA bound to uPAR is more efficient than free uPA in converting plasminogen to plasmin. By binding to the receptor, the activity of uPA is focused to the cell surface, and gives the cell the ability to efficiently degrade its surrounding matrix, which enables tumor cells to detach from the primary tumor and leads to tumor invasion and metastasis (Andreasen *et al.,* 2000).

The two natural uPA inhibitors, plasminogen activator inhibitor type 1 (PAI-1) and type 2 (PAI-2), belong to the serpin (serine protease inhibitor) family having an arginine in their reactive inhibitory center. They function by acting as pseudosubstrates and form an irreversible complex with their target protease. PAI-1 (M_r: approximately 50,000) is one of the main inhibitors of uPA and is a single-chain glycoprotein, inactivates both uPA and tPA (tissue-type plasminogen activator) by rapid formation of 1:1 complexes (Andreasen *et al.,* 2000). PAI-1 also binds to the extracellular matrix protein vitronectin with high affinity. Secreted PAI-1 as an unstable active inhibitor, is rapidly converted into its latent form unless it is stabilized by binding to vitronectin. Bound to vitronectin, PAI-1 stays active towards serine protease and can inhibit plasminogen activation by uPA at the cell surface (Conese and Blasi, 1995). PAI-2 (M_r: approximately 50,000) is also able to inhibit both uPA and tPA, although it reacts more slowly than PAI-1 (Rijken 1995).

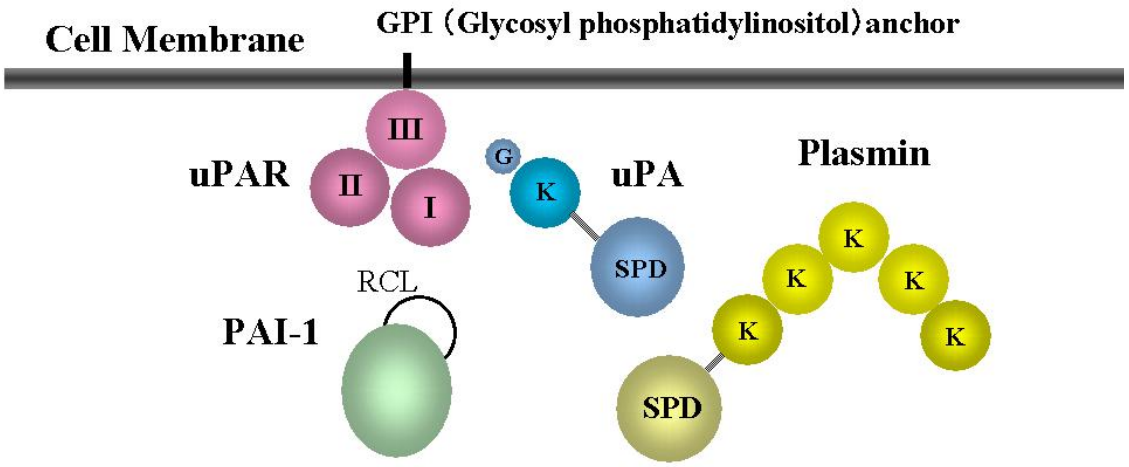

Figure 2. Schematic presentation of uPA, uPAR, PAI-1 and plasmin: uPA consists of a serine protease domain (SPD), a kringle domain (K), and a growth factor-like domain (G) harboring the uPAR binding site. uPAR has three domains and is attached to the cell membrane by a GPI anchor. The reactive center loop (RCL) of the inhibitor PAI-1 can bind to the active site of uPA, but PAI-1 can also interact with the extracellular matrix protein vitronectin to stay active towards serine proteases and to inhibit plasminogen activation by uPA at the cell surface. Plasmin also contains a serine protease domain as well and plus five kringle domains.

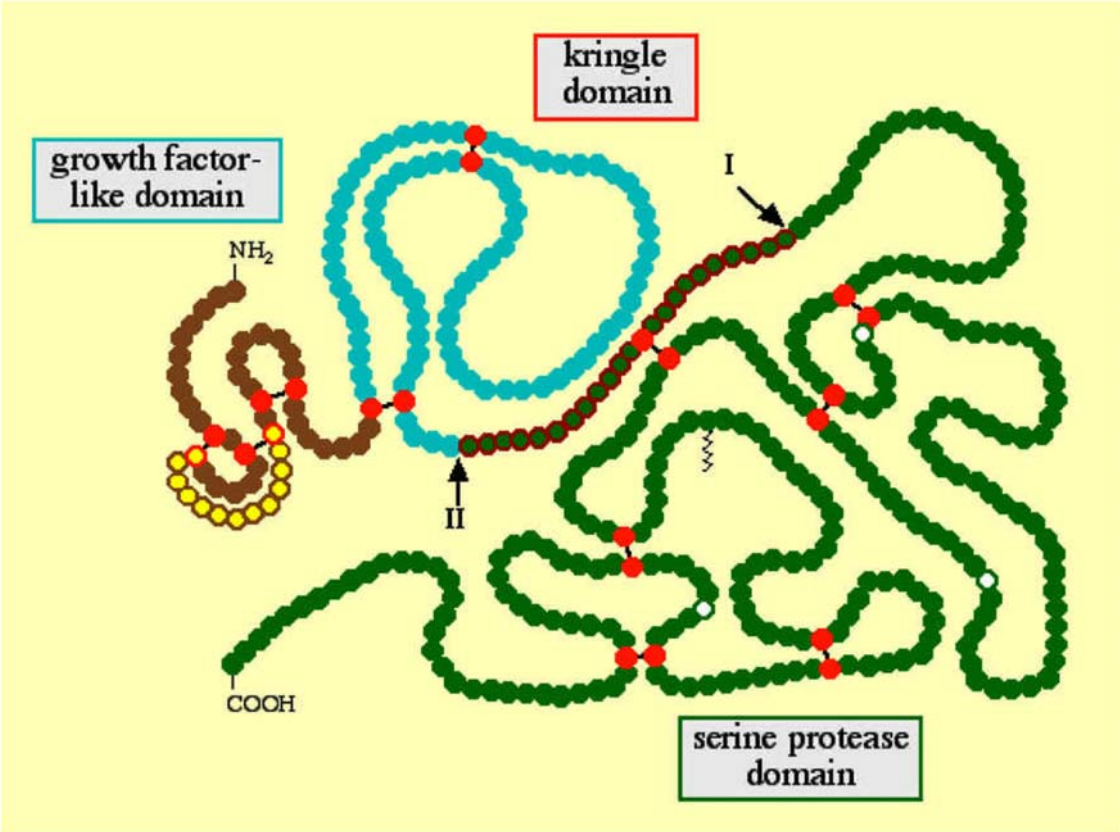

Figure 3. Domain structure of uPA: Schematic representation of the structure of uPA. The single-chain form of uPA, pro-uPA, is activated to the enzymatically active two-chain form, HMW-uPA, by cleavage of the Lys^{158}/Ile^{159} peptide bond (arrow I). The catalytic triad (His^{204}, Asp^{255}, Ser^{356}) within the C-terminal serine protease domain (green) is indicated in white. Further proteolytic cleavage within the N-terminal A-chain of uPA between Lys^{135}/Lys^{136} (arrow II) releases the so-called amino-terminal fragment (ATF), composed of the growth factor-like domain (GFD; brown) and the kringle domain (blue), and LMW-uPA. The uPAR-binding site of uPA (uPA_{19-31}) within the GFD is depicted in yellow. The peptide sequence $uPA_{136-158}$ (green dots with red margin), located between ATF and the B-chain (green), is called connecting peptide. The N-glycosylation site in the B-chain of uPA (Asn^{299}) is indicated by a zigzag line, cysteines involved in disulfide bridges are in red.

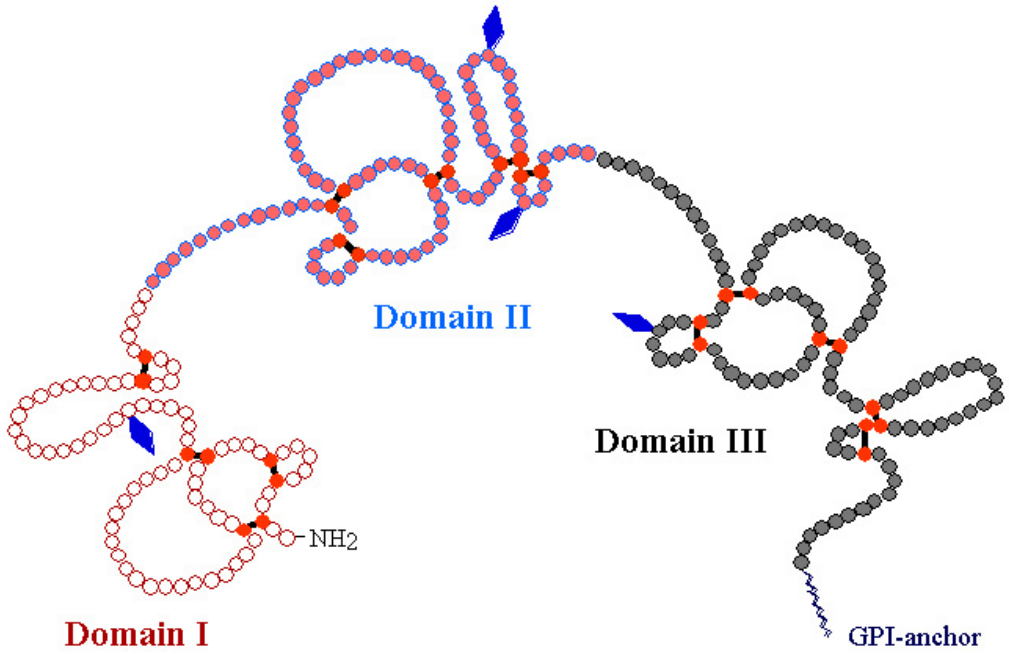

Figure 4. Domainic structure of the uPAR (CD87): uPAR consists of three homologous domains (I, II, and III, as numbered from the N terminus) and is anchored to the cell membrane by a glycosyl phosphatidylinositol (GPI)-anchor. The blue rhombus symbolizes N-glycosylation sites, cysteines involved in disulfide bridges are in red. Domain I is essential for uPA/uPAR interaction, however, the full-length three-domain uPAR molecule is required for high-affinity interaction with uPA.

A considerable number of studies have already shown that disruption of the interaction of uPA with uPAR leads to reduction of tumor invasion and metastasis (Muehlenweg *et al*., 2001, Reuning *et al*., 1998, Schmitt *et al*., 2000). It has been reported that competitive displacement of uPA from uPAR resulted in decreased proteolysis on the cell surface, which is the preferred site for uPA-mediated protein degradation (Crowley *et al*., 1993). Recombinant soluble form uPAR (suPAR) is also able to block binding of uPA to cell-surface-bound uPAR, the overexpression of suPAR showed profound

inhibitory effects on primary tumor growth, tumor spread, or experimental metastasis (Krüger *et al*., 2000, Lutz *et al*., 2001, Wilhelm *et al*., 1994). Various different experiments to interfere with the expression or reactivity of uPA or uPAR at the gene or protein level were performed successfully, including the use of antisense oligodeoxy-nucleotides, antibodies, inhibitors and recombinant or synthetic uPA and uPAR analogues (Kobayashi *et al*., 1995, Magdolen *et al*., 2001, Rabbani *et al*., 1995, Schmitt *et al*., 1995, Wilhelm *et al*., 1995). It was also shown that broad-spectrum serine protease inhibitors suppressed tumor growth and metastasis (Novak *et al*., 2005, Ohkoshi *et al*., 2002, Witschi *et al*., 1989).

Recently, several studies have been performed to identify and define new prognostic markers for the prediction of patients afflicted with solid malignant tumors. In a variety of malignancies including cancer of the breast, ovary, cervix, uteri, bladder, upper urogenital tract, kidney, head and neck, brain, lung, soft-tissue, stomach, colon, pancreas, esophagus, and liver, a strong prognostic impact has been attributed to components of the uPA-system: uPA, uPAR, and the two inhibitors PAI-1 and PAI-2 are statistically independent as prognostic factors (Duffy *et al*., 2001, Reuning *et al*., 1998, Schmitt *et al*., 2000).

In general, upregulation of the tumor antigen levels of uPA and/or PAI-1 is associated with poor disease outcome and tumor cell spread and metastasis (Grondahl-Hansen *et al*., 1993, Reuning *et al*., 1998, Schmitt *et al*., 2000). Especially, in breast cancer, determination of tumor antigen levels of uPA and PAI-1 is close to clinical routine to decide an individualized patients therapy (Duffy *et al*., 2002, Harbeck *et al*., 2002, Look *et al*., 2002). Additionally, increased levels of a soluble form of uPAR which are present in blood and ascites of patients with cancer of the ovary, lung, breast or colon, have also been associated with poor prognosis (Pedersen *et al*., 1993, Sier *et al*., 1998). In contrast to PAI-1, elevated PAI-2 antigen levels predict a good prognosis of cancer patients (Foekens *et al*., 1995). Thus the strong correlation between elevated tumor antigen levels and poor prognosis raises the possibility that plasminogen activation system has a key role in extracellular matrix degradation.

2.2 Competitive antagonist of uPA/uPAR-interaction derived from the uPAR binding site of uPA

Binding of (pro)-uPA to its cell surface receptor not only generates a pericellular proteolytic system, furthermore, surface-associated feedback-activation of pro-uPA by plasmin results in potentiation of proteolytic activity compared to activation in solution (Ellis *et al*., 1989). In addition to this, pro-forms of other proteolytic enzymes such as matrix metalloproteinases are activated by plasmin as well, allowing tumor cells to degrade the surrounding extracellular matrix. This matrix degradation facilitates cell migration and enables tumor cells to detach from the primary tumor and to spread to distant loci in the body (Andreasen *et al.*, 2000, Del Rosso *et al*., 2002, Reuning *et al*., 1998).

In contrast to uPAR in which different domains contribute to a composite uPA-binding site, the uPAR binding site within the uPA molecule encompasses a single continuous sequence within the GFD. Appella and coworkers demonstrated that a peptide comprising aa 12-32 of uPA (in which for technical reasons Cys^{19} was substituted by Ala) efficiently competed with ATF for binding to cell surface-associated uPAR. The rational for testing synthetic peptides derived from the N-terminal region of uPA originated from the finding that GFD binds with similar affinity to uPAR as do ATF and HMW-uPA, respectively. Moreover, ATF cleaved between Lys^{23}/Tyr^{24} or Phe^{25}/Ser^{26} does not interact with uPAR. A peptide encompassing aa 18-32 still competed with ATF for binding to uPAR, whereas a peptide spanning aa 9-20 including a Cys^{19} to Ala^{19} substitution had almost no effect, indicating that aa residues 20-30 of uPA, corresponding to the so-called loop B of GFD, confer receptor binding specificity (Appella *et al*., 1987).

NMR structural analysis of ATF (Hansen *et al*., 1994[1], Hansen *et al*., 1994[2]) revealed that the region Thr^{18}-Asn^{32} of uPA is folded into a flexible, seven-residue W-loop, i.e. a ring-like structure from Asn^{22} to Ile^{28}, that results from the double-stranded, antiparallel ß sheet between Thr^{18}-Ser^{21} and His^{29}-Asn^{32}. $Cys^{19}$and

Cys^{31}, although in close proximity, form disulfide bonds with other cysteines (Cys^{11}/Cys^{19} and Cys^{13}/Cys^{31}, respectively) (Fig. 5). Exchange of aa residues Lys^{23}, Tyr^{24}, Phe^{25}, Ile^{28}, or Trp^{30} by Ala in loop B of GFD led to a strongly reduced or even a complete loss of binding affinity towards uPAR. An Ala scan was also performed with the uPA derived synthetic peptide uPA_{14-32} (Magdolen *et al*., 1996). The individual replacement of aa 14-18, 20-23, 26-27, 29, or 32 by Ala had only minor effects on uPAR binding, whereas the individual substitution of Cys^{19}, Tyr^{24}, Phe^{25}, Ile^{28}, Trp^{30}, or Cys^{31} by Ala resulted in a considerable loss of uPAR binding activity. Interestingly, in the spatial structure of uPA, all of the side chains of Tyr^{24}, Phe^{25}, Ile^{28}, and Trp^{30} are displayed on one side of the ring-like structure, suggesting their involvement in specific hydrophobic interactions of uPA within the binding pocket of uPAR.

In order to determine the minimal uPAR binding region of uPA, a series of peptides with different lengths derived from wild-type uPA were tested for uPAR binding activity. By this, peptide uPA_{19-31} was found to compete with ATF for binding to uPAR, whereas peptides uPA_{18-30}, uPA_{20-32} or uPA_{20-30} were ineffective. Interestingly, uPA_{19-31} binds to uPAR with higher affinity than the longer peptides uPA_{14-32} or uPA_{16-32} (Bürgle *et al*., 1997). The results obtained with peptides derived from wild-type uPA are in agreement with the Ala-scanning experiments of uPA_{14-32}, defining Cys^{19} and Cys^{31} as the essential aa residues representing the N- and C-terminal borders of the uPAR binding epitope (Bürgle *et al*., 1997, Magdolen *et al*., 1996).

In uPA, Cys^{19} and Cys^{31} are not connected by a disulfide bond but are in close proximity (Fig. 5). The short distance between Cys^{19} and Cys^{31} in the native uPA molecule may explain, why the cyclic synthetic peptide $cyclo^{19,31}uPA_{19-31}$ in which Cys^{19} and Cys^{31} are linked by a disulfide bond, retain suPAR binding activity. The disulfide-bridged form of $uPA_{19–31}$ displays an IC50-value similar to that of its corresponding linear form (IC50: ~ 700 nM) (Bürgle *et al*., 1997). The distance between the Ca-atoms at aa positions 19 and 31 was further narrowed down from 6.1 Å in native uPA and 5.2 Å in $cyclo^{19,31}uPA_{19-31}$ to about 4.8 Å by generation of another peptide variant, $cyclo^{19,31}[Ala^{19}$-S-$Ala^{31}]$-uPA_{19-31}, in which the cystine [Cys^{19}-Cys^{31},

which formally corresponds to Ala^{19}-S-S-Ala^{31}] was substituted by lanthionine [Ala^{19}-SAla^{31}]. This peptide (cyclo^{19,31}[Ala^{19}-S-Ala^{31}]-uPA_{19-31}) still interfered with uPA/uPAR interaction but exhibited an about 10-fold lower inhibitory activity than the parent peptide cyclo^{19,31}-uPA_{19-31} (Magdolen *et al*., 2001).

A systematic D-aa scan was performed, in which each of the 13 L-aa of cyclo$^{19,31}uPA_{19-31}$ was individually substituted by the corresponding D-aa (Magdolen *et al*., 2001). This led to the identification of cyclo^{19,31}[D-Cys19]-uPA_{19-31} (WX-306) as a potent inhibitor of uPA/uPAR interaction (Fig. 5), displaying an only 20 to 40-fold lower binding capacity (IC50: ~ 200 nM) than the naturally occurring uPAR ligands uPA and ATF (IC50: ~ 5-10 nM). As one can see in figure 5, the switch of the cysteine bridges to produce cyclo$^{19,31}uPA_{19-31}$ requires a change of the Cys side chain orientation, which is achieved by change in chirality. In addition to the uPA derived peptides with single D-aa substitutions, a cyclic peptide was synthesized in which all L-aa were substituted by their corresponding D-enantiomers and in which all of the peptide bonds were inverted. This so-called retro-inverso, protease-insensitive cyclo^{19,31}-uPA_{19-31}-peptide did not show any uPAR binding activity. Several reasons for the lack of binding activity of the retro-inverso peptide are conceivable:

i) Retro-D-peptides harbor exchanged N- and C-termini; the terminal groups in cyclo$^{19,31}uPA_{19-31}$ may be important for the receptor-ligand interaction with uPAR. One has to consider that in a cyclic retro-inverso peptide, the side chain orientation is different from that in the parent peptide (Wermuth *et al*., 1997).

ii) The amide bonds in the backbone of the peptide (which are reversed in the retro-inverso peptide) may be necessary for uPAR binding.

iii) The hydrogen bond pattern in retroinverso peptides is different from that of the parent peptides.

A series of cyclic peptides was synthesized in which certain aa of cyclo$^{19-31}uPA_{19-31}$ were deleted and/or replaced by other aa (Bürgle *et al*., 1997, Guthaus *et al*., 2002, Schmiedeberg *et al*., 2002). Since - in addition to Cys^{19} and Cys^{31}- Lys^{23}, Tyr^{24}, Phe^{25}, Ile^{28}, and Trp^{30}, respectively, have been proven to be important determinants of uPAR

binding (Magdolen *et al*., 1996), mainly disulfide-bridged cyclic peptides of different ring sizes were synthesized encompassing those aa. Among them, only the decameric peptide cyclo^{21,29}uPA$_{21-30}$[S21C;H29C] inhibited uPA/uPAR interaction displaying an IC50 of ~ 900 nM (IC50 of cyclo$^{19-31}$uPA$_{19-31}$: ~ 700 nM) (Guthaus *et al*., 2002, Schmiedeberg *et al*., 2002). The systematic substitution of each aa residue in cyclo^{21,29}uPA$_{21-30}$[S21C;H29C] by Ala indicated that the side chains of Cys^{21} and Cys^{29} (leading to linear peptides), Tyr^{24}, Phe^{25}, Ile^{28}, and Trp^{30}, respectively, are essential for uPAR binding (Schmiedeberg *et al*., 2002). In addition, the impact of modification of the stereochemical orientation of individual aa side chains in cyclo^{21,29}uPA$_{21-30}$[S21C;H29C] on uPAR binding activity was analyzed. Derivatives of cyclo^{21,29}uPA$_{21-30}$[S21C;H29C] harboring either D-Tyr^{24}, D-Phe^{25}, or D-Ile^{28} did not elicit uPAR binding activity. The peptide variant containing D-Trp^{30} displayed an about three times weaker uPAR binding activity than the lead peptide with L-Trp^{30} in the C-terminal position. This may be explained by the rotational freedom of the exocyclic aa enabling the aromatic side chain to adopt the conformation required for uPAR binding. Substitution of L-aa in cyclo^{21,29}uPA$_{21-30}$[S21C;H29C] by D-aa at positions Asn^{22}, Lys^{23}, Ser^{26}, and Asn^{27}, respectively, yielded peptides with strongly reduced uPAR binding affinity. This finding indicates that stereochemical inversion of most side-chain residues in cyclo^{21,29}uPA$_{21-30}$[S21C;H29C] reduces uPAR binding affinity, regardless of whether the corresponding aa side chains are required for receptor binding or not. Stereochemical modification at Cys^{21}, yielding cyclo^{21,29} [D-Cys21]uPA$_{21-30}$[S21C;H29C] (WX-360) (Fig. 5), displayed a much higher uPAR binding activity (IC50: ~ 40 nM) than its L-isomer (~ 900 nM). This finding is in agreement with that for cyclo^{19,31}[D-Cys19]-uPA$_{19-31}$ in which the introduction of D-Cys at position 19 resulted in a more active peptide (IC50: ~ 200 nM versus ~ 700 nM).

The inversion of the stereochemical orientation of Cys^{21} in the smaller cyclic peptide cyclo^{21,29}uPA$_{21-30}$[S21C;H29C] led to an even more pronounced effect regarding uPAR binding activity as compared to the exchange of L-Cys^{19} by D-Cys in cyclo^{19,31} uPA$_{19-31}$. The resulting high-affinity uPA mimic peptide displays a binding reactivity to

cellular uPAR (IC50: ~ 40 nM) that is only 4-8 times weaker than that of the natural ligand uPA (IC50: ~ 5 - 10 nM). Thus, cyclo^{21,29}[D-Cys21]uPA$_{21-30}$[S21C;H29C] (WX-360) represents one of the most active synthetic uPAR antagonists known to date (Schmiedeberg *et al*., 2000, Schmiedeberg *et al*., 2002).

Efforts have been undertaken to reduce the *in vivo* proteolytic degradation of cyclo^{21,29}[D-Cys21]uPA$_{21-30}$[S21C;H29C] (WX-360). For this purpose, the Lys residue of cyclo^{21,29}uPA$_{21-30}$[S21C;H29C] was individually replaced by several nonnatural aa such as norleucine (Nle), ornithine, diaminobutyric acid, or diaminopropionic acid. The Nle-variant, cyclo^{21,29}[D-Cys21]-uPA$_{21-30}$[S21C;K23Nle;H29C] (WX-360-Nle), exerts similar binding affinities (IC50: ~ 70 nM) as cyclo^{21,29}[D-Cys21]uPA$_{21-30}$ [S21C;H29C] (WX-360). Both cyclo^{21,29} [D-Cys21]uPA$_{21-30}$[S21C;H29C] (WX-360) and cyclo^{21,29}[D-Cys21] -uPA$_{21-30}$[S21C;K23Nle;H29C] (WX-360-Nle) were highly resistant to proteolytic degradation in human and rodent plasma or serum when compared to other uPA-derived peptides lacking a non-natural D-aa (e.g. cyclo^{19,31}-uPA$_{16-32}$). The Nle-variant WX-360-Nle was completely resistant to plasmin-mediated proteolysis, whereas cyclo^{21,29}[D-Cys21] uPA$_{21-30}$[S21C;H29C] (WX-360) was readily degraded (Schmiedeberg *et al*., 2002).

The two peptides, WX-360 and WX-360-Nle were tested in *in vivo* nude mice model for their potency to inhibit tumor growth and intraperitoneal spread.

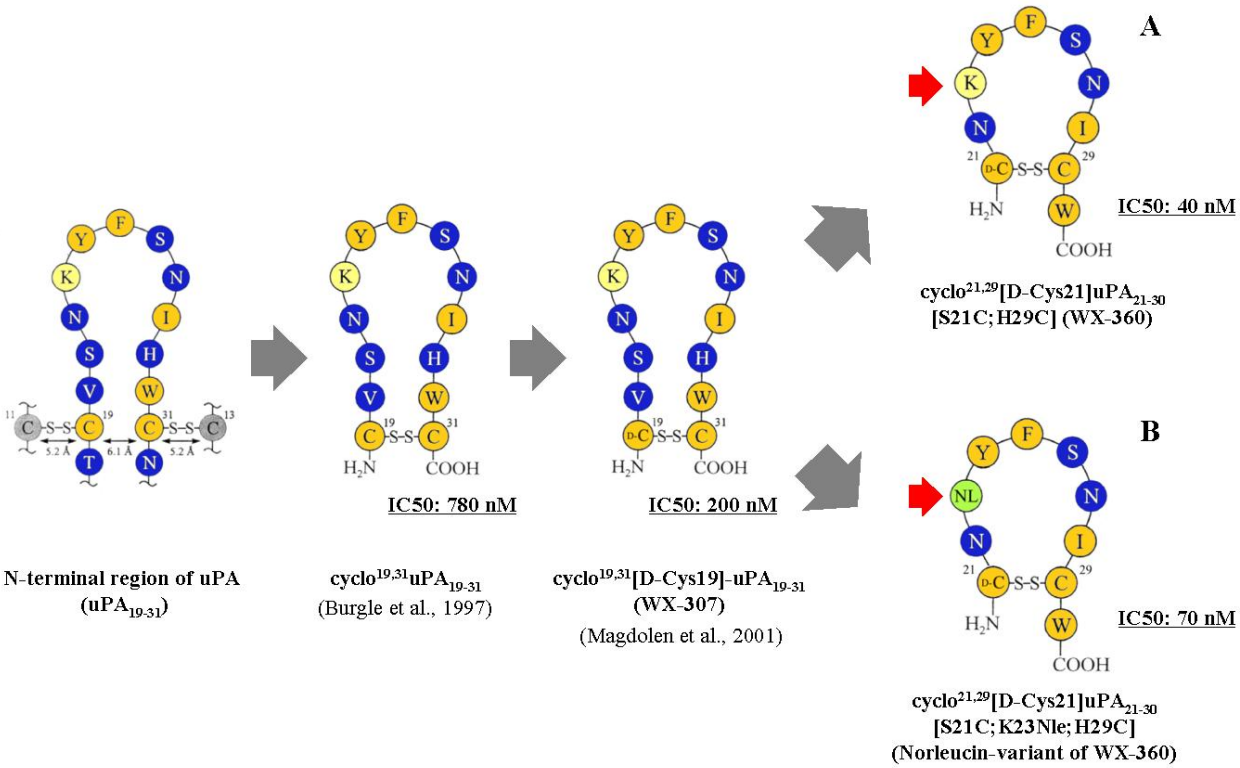

Figure 5. Structures of the synthetic cyclic uPA-derived peptide WX-360 (cyclo^{21,29}[D-Cys21]-uPA$_{21–30}$[S21C;H29C]) (A) and its norleucine derivative WX-360-Nle (cyclo^{21,29}[D-Cys21]-uPA$_{21–30}$[S21C;K23Nle;H29C]) (B): WX-360 was designed using cyclo^{19,31}[D-Cys19]-uPA$_{19-31}$ (WX-307) as the lead structure, which was developed based on the uPA$_{19-31}$: uPAR-binding site of uPA. To prolong the *in vivo* half-life, a norleucin-variant of WX-360 was constructed (exchange of K23 by Nle), exerting a similar binding affinity as WX-360. The red arrows point to the lysine residue (K23) in WX-360 and norleucine (Nle23) in WX-360-Nle, respectively.

3. Materials and Methods

3.1 Reagents

Two synthetic cyclic peptides have been developed based on the lead structure WX-307 (cyclo^{19,31}[D-Cys19]-uPA$_{19-31}$) (Magdolen *et al*., 2001): WX-360 (cyclo^{21,29}[D-Cys21] uPA$_{21-30}$[S21C;H29C]) and its derivative WX-360-Nle (cyclo^{21,29}[D-Cys21]-uPA$_{21-30}$ [S21C;K23Nle;H29C]), in which lysine 23 is substituted by norleucine (Guthaus *et al*., 2002, Schmiedeberg *et al*., 2002) and was obtained from Wilex AG (Munich Germany).

3.2 Cell lines

OvMz-6 was originally established from a patient with advanced serous cystadenocarcinoma of the ovary (Möbus *et al*., 1994), typically induce a large primary tumor and abundant intraperitoneal metastases. MDA231 and MCF-7 are mammary adenocarcinoma cell line, established from a pleural effusion of a patient. ZR75 is invasive ductal adenocarcinoma of breast cancer, derived from an ascites of a patient, MCF10a human immortalized breast epithelial cells in a fibrocystic disease (ATCC, Rockland, USA).

OvMz-6 cells were transfected with the bacterial *lacZ* gene which encodes for ß-galactosidase (OvMz-6-BAK) and, thus, the resulting cells can be stained with the ß-galactosidase substrate 5-bromo-4-chloro-3-indolyl ß-D-galactoside (X-Gal) (Roche Diagnostics, Mannheim, Germany) (Fig. 6) in order to follow spreading of tumors in *in vivo* models (Krüger *et al*., 1998).

Cells were cultured to 80 % confluence in T-25 cell culture flasks (Becton Dickinson, Heidelberg, Germany) in DMEM medium supplemented with 10 mM HEPES, 10 % fetal bovine serum, 200 mM L-glutamine (Gibco BRL, Eggenstein, Germany), and antibiotics (penicillin/streptomycin) (Biochrom KG, Berlin, Germany) at 37 ^{o}C in humidified atmosphere containing 5 % CO_2/95 % air. In case of MCF10a, DMEM

/F-12 medium supplemented with 10 mM HEPES, 5 % fetal bovine serum, 10 µg/ml Insulin (Gibco BRL, Eggenstein, Germany), 20 ng/ml epidermal growth factor (Promega, Mannheim, Germany), 0.5 µg/ml hydrocortisone (Sigma, Munich, Germany), and antibiotics (penicillin/streptomycin) (Biochrom KG, Berlin, Germany). Cells were routinely propagated by using 0.05 % EDTA (Biochrom KG, Berlin, Germany) in phosphate-buffered saline (PBS), and added 0.125% Trypsin (Biochrom KG, Berlin, Germany) for MCF10a.

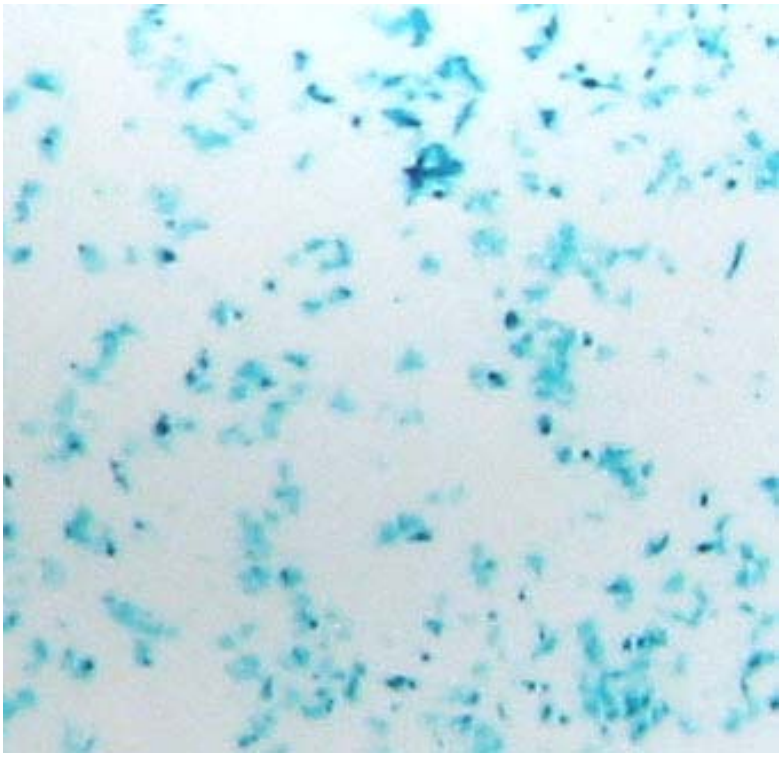

Figure 6. X-Gal staining of *lac Z*–transfected cells: The bacterial ß-galactosidase *lacZ* gene is frequently used to genetically recognize tumor cells. The expression of transgenic constructs can be monitored by the chromogenic substrate X-Gal, which is converted into a blue color to allow visualization of disseminated tumor cells *in vivo*.

3.3 uPA, uPAR and PAI-1 ELISA

Expression of uPA, uPAR and PAI-1 in OvMz-6-BAK cells and its parent cell lines was investigated using ELISAs.

ELISAs for uPA and PAI-1 were obtained from American Diagnostica GmbH (Pfungstadt, Germany), IMUBIND uPA ELISA kit #894, IMUBIND PAI-1 ELISA kit #821 respectively. The uPAR antigen was kindly estimated by Dr. Mathias Kotzsch (Institute of Pathology in TU-Dresden, Germany) (Kotzsch *et al.*, 2000). The protein content of the cell extracts was determined by the BCA protein assay reagent kit.

7.0×10^5 cells were suspended in 1 mL of the supplemented medium, seeded on 24-well plates, and incubated for 24 h. After this incubation, the medium was exchanged and incubated for more 24 h. The cell medium was removed and centrifuged (10 min, 12,000 x g, 4 °C). The supernatant was collected for determination of uPA and PAI-1 antigen. For preparation of cell extracts, the cells were incubated in 400 µl TBS, 1 % Triton X-100, 3 h with gentle shaking, the solution collected and centrifuged (30 min, 12,000 x g, 4 °C). The amount of uPA and PAI-1 was also estimated in the cell culture supernatant. Concerning the uPAR ELISA, approximately 2.0×10^6 cells (80 % confluence), were collected from cell culture flasks.

Mouse tumor tissue extracts were prepared by suspending pulverized tissues, previously frozen in liquid nitrogen, in Trisbuffered saline (TBS), followed by centrifugation (30 min, 12000 x g, 4 °C). Supernatants of this non-detergent extraction were subjected to uPA, PAI-1 and uPAR antigen measurement by ELISA.

3.4 Proliferation assay

Growth curves of OvMz-6 were taken to compare with human carcinoma cell lines, MCF7, MDA231, ZR75, and human immortalized breast epithelial cells MCF10a. Initially, 15,000 cells in 1ml 10 % FCS DMEM medium were seeded in the wells of 24-well plate and incubated for 48 to 96 h. After incubation cells were washed with PBS, detached from the plate using 0.05 % EDTA solution and counted in hemocytometer upon Trypan blue exclusion. Experiments were repeated 4 times in triplicates.

3.5 Invasion assay

Invasion assays were performed using inserts (Becton Dickinson, Heidelberg, Germany) incorporating polyethylene terephthalate (PET) track-etched membranes, 8mm pore size. Aliquots of Matrigel (11.3 mg/ml, Becton Dickinson Labware, Bedford, MA) were stored frozen at –20 ^{o}C. After thawing on ice overnight the Matrigel was diluted 1:24 with cold PBS and the upper side of the filters was coated with Matrigel per insert. By testing different concentrations of Matrigel, it was found that 70 µl per filter gave the best resolution of the invasive capacity of the cells. The plates were incubated for 3 h at 37 ^{o}C in a cell culture incubator. After gelling the Matrigel was dried overnight in uncovered plates in a laminar hood. The next day, the gel was rehydrated for 2 h by addition of 200 µl serum-free DMEM/0.1 % BSA. Cells were grown until 60 to 80 % confluency and adjusted to 10^5 cells/ml DMEM/0.1 % BSA. 5 x 10^4 cells/500 µl medium were seeded into each insert. The lower chambers of the inserts were filled with 750 µl DMEM containing 10 % FCS as a chemoattractant. After 96 hours of incubation the Matrigel with the noninvaded cells was removed with Kimwipes and invaded cells on the lower side of the filter were fixed and stained using Diff-Quick (Dade Behring AG, Switzerland). The stained cells were counted under a light microscope with the help of a grid. Based on the growth curve of proliferation assay, the time when 100 cells invade the Matrigel layer was calculated. The Experiments were repeated 4 times in triplicates.

3.6 Adhesion assay

Fibronectin (Becton Dickinson, Heidelberg, Germany), vitronectin (Promega, Germany), collagen type IV and Laminin (Sigma, Munich, Germany) were diluted with PBS and added to each well of a 96-well plate (the final concentration of 10 µg/ml). After overnight incubation at 4 ^{o}C, wells were washed two times with PBS, blocked with PBS/2 % BSA for 3 h at RT and again washed with PBS. 40,000 cells in 100 µl DMEM/0.5 % BSA were seeded to each well, the plate was incubated for 2 h at 37 ^{o}C. Non-adherent cells were carefully removed by washing with PBS, the adherent cells were quantified by determining the activity of the ubiquitous lysosomal enzyme N-acetyl-ß-D-hexosaminidase by incubating them with substrate solution (50 µl/well + 50µl/well PBS) for 1 h at 37 ^{o}C. The resulting color reaction was stopped with the stop solution and the absorbance measured at 405 nm. The serial dilutions of cell suspensions in the range of 2,500 to 40,000 cells in 50 µl PBS served as the standard values of the measurements. Assays were performed 4 times in triplicate.

3.7 Animal model

Pathogen-free female athymic (*nu/nu*) mice (4-6 weeks old) were obtained from Charles River Laboratories (Sulzfeld, Germany). 3.0 x 10^7 OvMz-6-BAK cells were suspended in 500 µl PBS and inoculated into the peritoneal cavity of nude mice. These mice were divided into three groups, which either received WX-360, WX-360-Nle (20 mg/kg/day, respectively), or vehicle only (5 % mannitol, 0.6 % DMSO) in a blinded manner. The peptides or the vehicle only were injected intraperitoneally once per day for 37 days (treatment started one day post-inoculation). At the end of the study, the mice were sacrificed, all intraperitoneal organs removed and stained with X-Gal in order to facilitate identification of the spreading tumor cells. Tumor tissue was partly snap frozen in liquid nitrogen for the evaluation total protein levels of selected markers (uPA, uPAR, PAI-1) by ELISA. The internal organs were washed in ice-cold PBS, fixed (1 hour in 2 % formaldehyde, 0.2 % glutaraldehyde solution), washed three times in ice-cold PBS, and then incubated in X-Gal solution containing 5 mmol/L $K_3[Fe(CN)]_6$, 5 mmol/L $K_4Fe(CN)_6 \cdot 3H_2O$, 2 mmol/L $MgCl_2$, 0.01 % sodium

desoxycholate, 0.02 % NP40, and 1 mg/mL X-Gal (3 to 4 h, 37 ^{o}C) and then overnight at 4 ^{o}C (Krüger *et al*., 1998). To account for weight differences between individual mice, we determined the relative tumor mass within the total situs. To achieve this, we removed all intraperitoneal organs including the tumor and weighed this as the total situs, and then, we separated all visible tumor mass from them (see Fig. 4). The data are presented as the ratio between tumor mass over the weight of the total situs (Lutz *et al*., 2001). Finally, the blinded code was uncovered and statistical analyses performed.

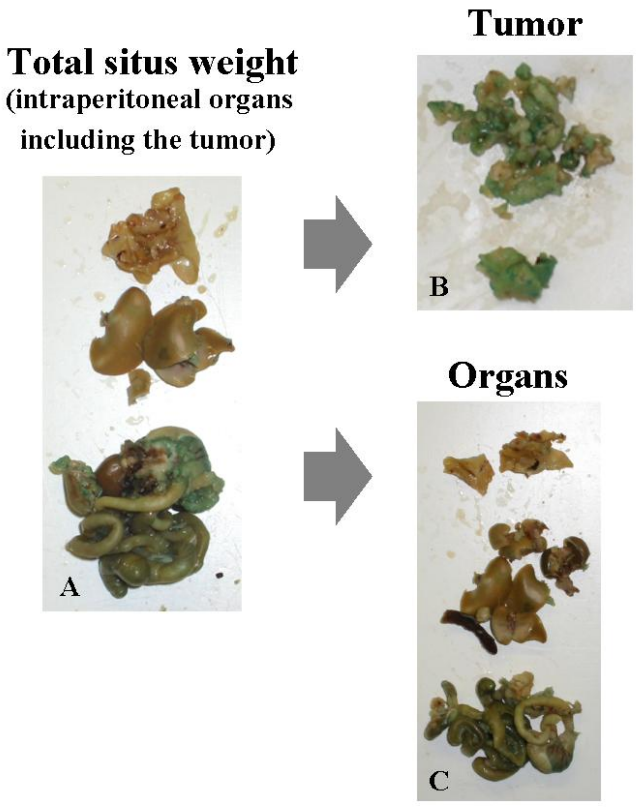

Figure 7. Ratio between tumor mass weight and the weight of total situs: All intraperitoneal organs (heart, liver, lung) (A) including the tumor were removed as the total situs. Then, all visible tumor mass was excised, and subsequently weighed (B). The data are presented as the ratio of tumor weight over total situs weight.

3.8 Statistical analyses

Significant differences in the tumor weight between mice were calculated using Student's t-test owing to normal distribution of the data. Concerning data on tumor weight over total situs weight, the normal distribution Student's t-test was not applicable; therefore, a Kruskal-Wallis one-way analysis and Dunn's multiple comparison test were performed to investigate for differences between the three groups. A significance level of $p < 0.05$ was considered statistically significant.

4. Results

4.1 Determination of uPA, PAI-1 and uPAR by ELISA

OvMz-6 cells are known to grow locally invasive and to form liver metastasis. The amount of uPA, PAI-1, and uPAR antigens in the cell extracts and conditioned medium was determined by specific ELISAs. The measurements demonstrated that the *lacZ*-tagged cell line OvMz-6-BAK shows high expression levels of uPA (7.2 ng/mg, 0.97 ng/mL in the cell extract and culture medium, respectively) and PAI-1 (11.9 ng/mg, 23 ng/mL in the cell extract and culture medium, respectively) (Table 1). For uPAR ELISA, two different antibody, HU/IIIF10 and HU/HD13 were applied which measure different forms of uPAR (Kotzsch *et al.*, 2000). In case of OvMz-6-BAK, we also found high level of uPAR, 3.34 ng/mg (HU/IIIF10) and 1.5 ng/mg (HU/HD13) in the cell extract (Table 1). These expression levels in OvMz-6-BAK were not significantly different from those of the parent cell line. Results may indicate that the tumor growth and metastasis of OvMz-6 strongly depend on urokinase plasminogen activation system.

4.2 Characterization of proliferation of OvMz-6 cell lines

Proliferation of OvMz-6 cells was tested under the normal conditions, in DMEM medium supplemented with 10 % fetal bovine serum, at 37 ^{o}C in humidified atmosphere containing 5 % CO_2/95 % air. Cells were subcultured in 24-well plate, for 48 and 96 h, to compare the growth rate. In addition to OvMz-6 cells, proliferation of MCF7, MDA231, ZR75, human mammary carcinoma cells and MCF10a human immortalized breast epithelial cells were also determined. As shown in Figure 8, OvMz-6 cells showed fastest proliferation, grew 1.5 times faster than ZR75 cells, and 3 times than MDA231 cells. Especially those cells showed a fast growth rate after 48 h.

Cell line	uPA		PAI-1		uPAR	
	Cell extract (ng/mg protein)	Culture mdium (ng/ml)	Cell extract (ng/mg protein)	Culture mdium (ng/ml)	Cell extract (HU/IIIF10) (ng/mg protein)	Cell extract (HU/HD13) (ng/mg protein)
OvMz-6-BAG	7.2	0.97	11.9	23	3.34	1.5
OvMz-6	8.12	2.77	17.5	32.3	4.66	1.96

Table 1. Determination of uPA, PAI-1 and uPAR by ELISA: Antigen levels were determined in cell extracts and in spent conditioned medium, 24 h after exchange of medium. Assays were performed in triplicate and data shown are representative results. All determinations were performed at least in duplicate and the average numbers are given. The antigen content in cell extracts is expressed in ng/mg protein and in the cell culture medium as ng/ml. Concerning uPAR antigen detection, the following ELISA kits were used, (1); HU/IIIF10 ELISA with epitope-defined monoclonal antibody IIIF10 against domain I of uPAR, (2); HU/HD13 ELISA with conformation-dependent monoclonal antibody HD13.1 against domain II and III. (Kotzsch *et al*., 2000).

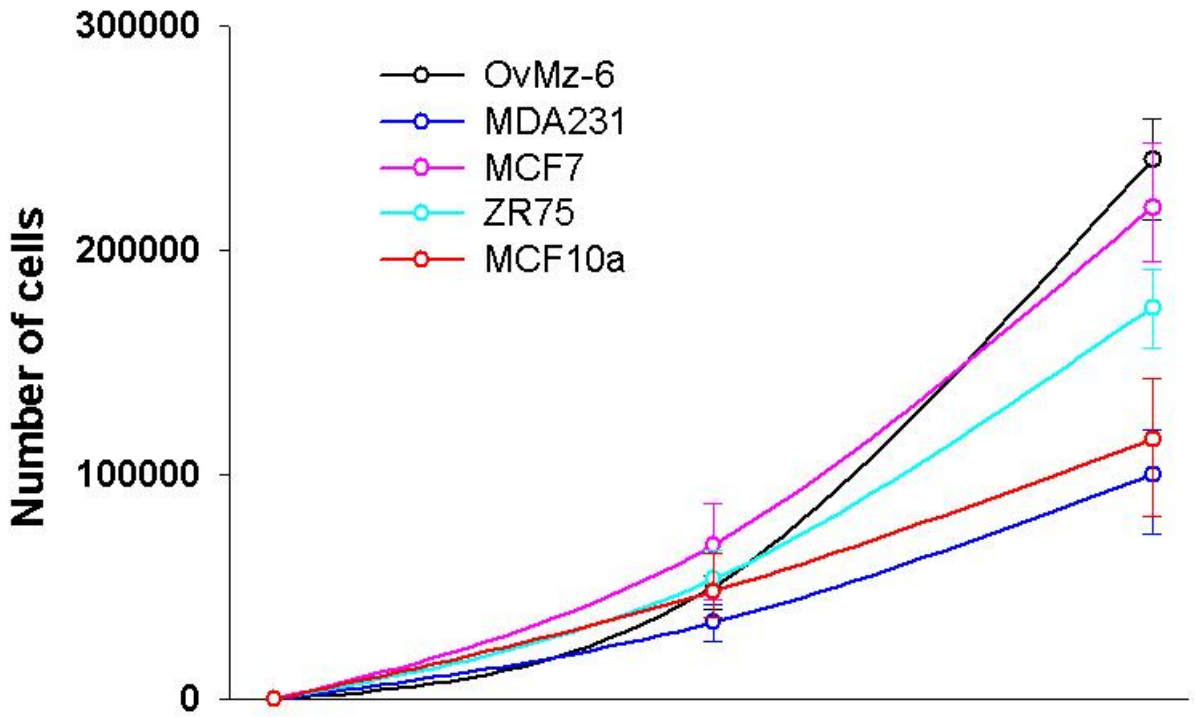

Figure 8. Proliferation of human carcinoma cells OvMz-6, MCF7, MDA231, ZR75, and MCF10a human immortalized breast epithelial cells: Proliferation of each of these cell lines was tested by seeding of 15,000 cells in 1 ml DMEM, 10% FCS into wells of a 24-well plate. After 48 or 96 h of incubation, cells were counted with Trypan blue exclusion. Four independent experiments were performed in triplicate. Mean values ± SD are indicated.

4.3. Invasive capacity of OvMz-6 cells

To test for the in vitro invasive capacity of OvMz-6, we performed an assay using Matrigel as the extracellular matrix. Cells were placed into the upper compartment of an invasion chamber on top of an insert, the lower compartment was filled with DMEM containing 10 % FCS as a chemoattractant. After 48 h to 96h, the cells on the lower side of the filter were counted and the time when 100 cells penetrate the Matrigel-coated filter was calculated. In addition to OvMz-6 cells, MDA231, ZR75 human mammary carcinoma cells and MCF10a human immortalized breast epithelial cells were also used for comparison. As can be seen in Figure 9, OvMz-6 cells were effectively in penetrating the Matrigel barrier especially compared to non-malignant MCF10a cells. It was shown that OvMz-6 cells are much more invasive than MDA231 cells which it has already known that are spontaneously metastasizing mammary carcinoma to the liver, lung and brain.

4.4 Biological activity of OvMz-6 in cell adhesion assay

To analyze the adhesive characteristics, OvMz-6, MCF7, MDA231, ZR75, human carcinoma cells are seeded into wells of microtiter 96-well plate precoated with fibronectin, vitronectin, collagen type IV or Laminin. The adherent cells were quantified by determining the activity of the ubiquitous lysosomal enzyme N-acetyl-ß-D-hexosaminidase by incubating them with substrate solution. OvMz-6 cell lines showed the strongest adhesion to vitronectin, on the other hand, the weakest to Collagen IV in 4 human carcinoma cell lines (Fig. 10). Concerning the adhesion to Laminin, ZR75 exhibited adhesive characteristics more than OvMz-6 and MDA231 cells, which is consistent with the results of Matrigel invasion assay. Since Laminin is the main component of Matrigel, the adhesion to Laminin might contribute to the invasive capacity.

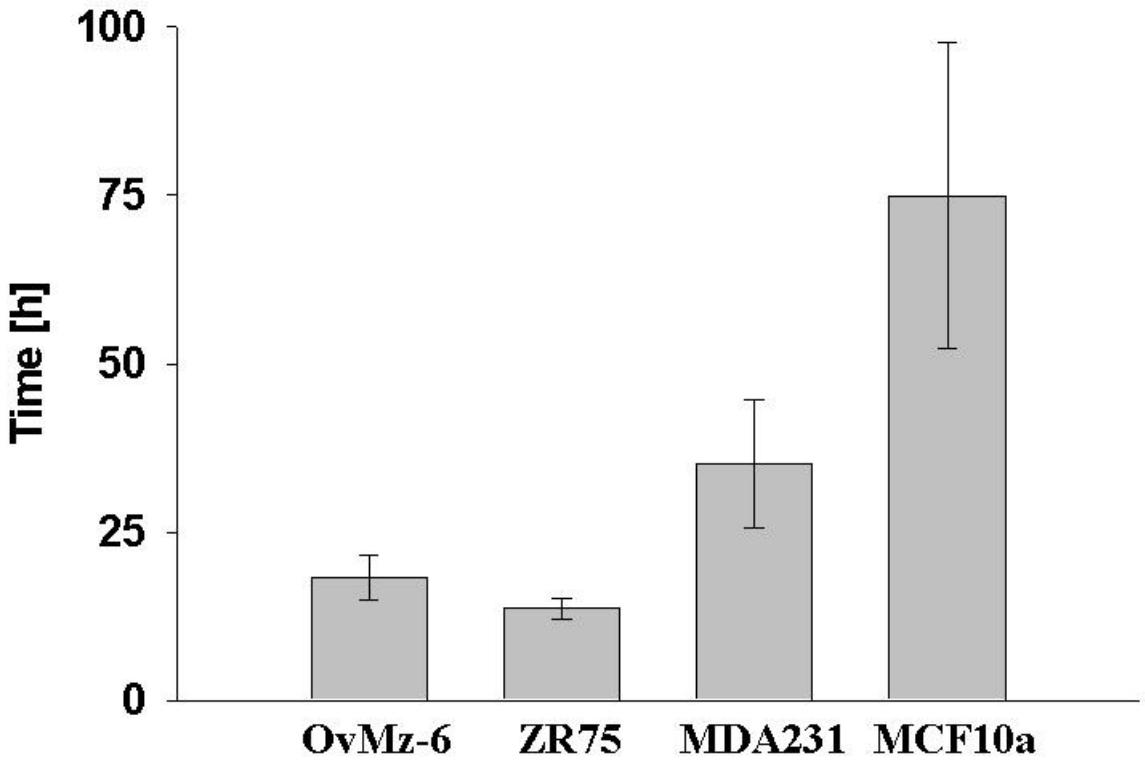

Figure 9. Matrigel invasion by human carcinoma cells OvMz-6, MDA231, ZR75 and MCF10a human immortalized breast epithelial cells: 80 % confluent cells were placed into the upper compartments of the invasion chambers (5 x 10^4 cells in 500 µl of 0.1 % BSA/DMEM). The lower chambers of the inserts were filled with 750 µl DMEM containing 10 % FCS as the chemoattractant. After 48 to 72 h of incubation, the Matrigel layer of the upper compartment was removed, the invaded cells on the lower side of the filter were fixed, stained, and counted. Based on the growth curve established by the proliferation assay, the time when 100 cells invade the Matrigel layer was calculated. The experiments were performed 4 times in triplicate, mean values ± SD are indicated.

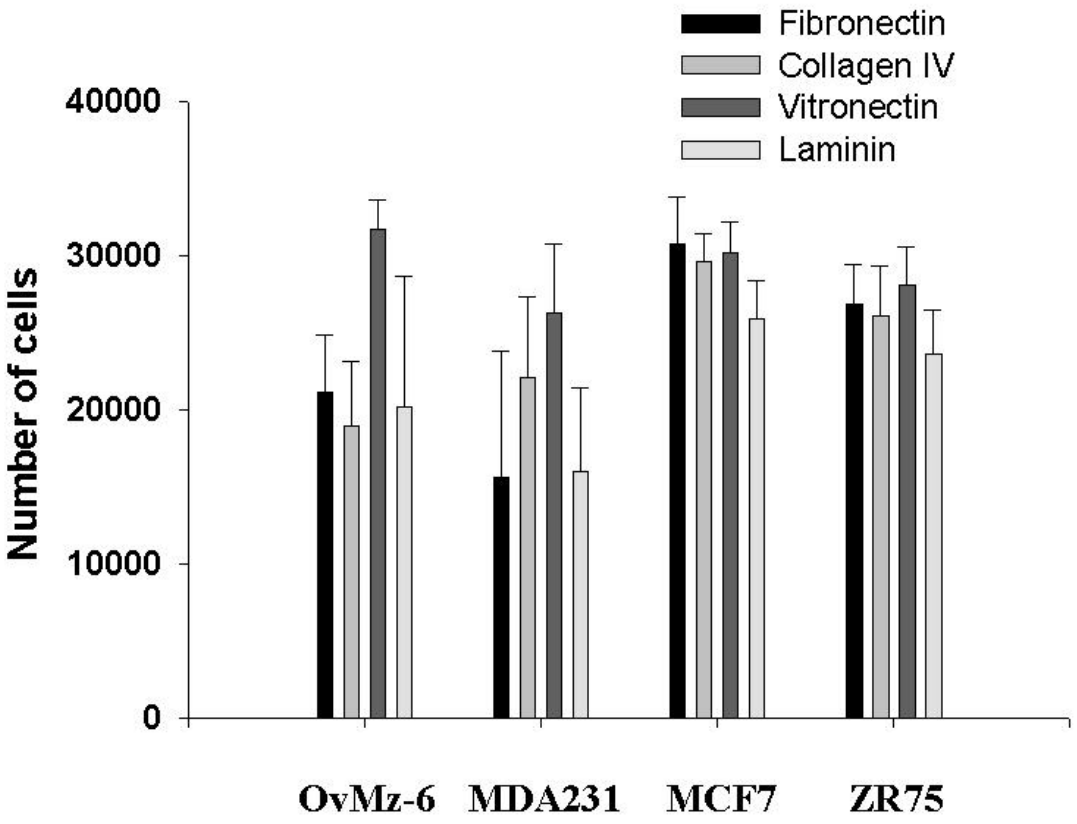

Figure 10. The adhesive characteristics of human carcinoma cells. 40,000 cells were seeded into the wells of a 96-well plate pre-coated with vitronectin, fibronectin, collagen type IV or Laminin. After 2 h of incubation, non-adherent cells were received in PBS and the remaining cells incubated with a hexoaminidase substrate solution. The absorbance of the color reaction was measured at 405 nm. Serial dilutions of cell suspensions in the range of 2,500 to 40,000 cells in 50 µl PBS served as the standard values of the measurements, thereby the number of adherent cells is calculated. Assays were performed 4 times in triplicate, mean values ± SD of independent experiments are indicated.

4.5 Effect of synthetic cyclic competitive uPA-derived peptide WX-360 and WX-360-Nle in vivo

uPA/uPAR-interaction via the specific sequence within the N-terminal region of uPA (uPA19-31) directs the proteolytic step in tumor cell proliferation, invasion and metastasis. Synthetic cyclic peptides, derived from the uPAR-binding sequences within the N-terminal region of uPA (uPA_{19-31}), were applied and tested whether such competitive antagonists of uPA/uPAR-interaction reduce tumor burden of a human ovarian carcinoma in *nude* mice (Fig. 11).

WX-360 (cyclo^{21,29} [D-Cys21]-uPA_{21-30} [S21C;H29C]) is a competitive peptide antagonist of the uPA/uPAR interaction derived from receptor binding region of uPA. This peptides display an only five to ten-fold lower affinity to uPAR (IC50: ~ 40 nM) as compared to the naturally occurring uPAR-ligand uPA. Furthermore, as WX-360 harbors a lysine residue (K^{23}) and, thus, a target site for serine proteases such as plasmin, K^{23} was replaced by the non-protein amino acid norleucine. This derivative WX-360-Nle (cyclo^{21,29}[D-Cys21] -uPA_{21-30} [S21C;K23Nle;H29C]), still displays high binding affinity (IC50: ~70 nM).

In this study, WX-360 and WX-360-Nle were tested in nude mice for their potency to inhibit tumor growth and intraperitoneal spread of *lacZ* tagged human ovarian cancer by inhibiting the binding of uPA to uPAR.

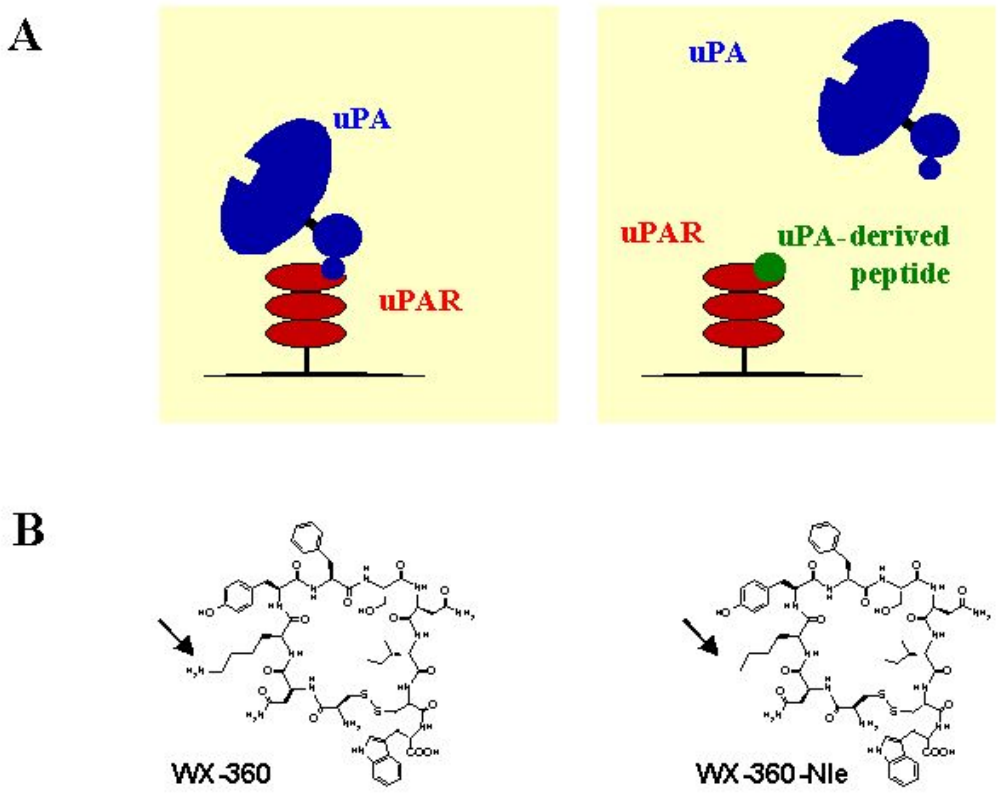

Figure 11. Competitive antagonists of uPA/uPAR-interaction. (A) Binding of uPA to the tumor cell surface (uPAR, CD87) facilitates tumor cell proliferation, invasion, and metastasis (del Rosso *et al*., 2002, Magdolen *et al*., 2001). uPA binds to uPAR by the peptide sequence uPA_{19-31}. Based on this sequence, small cyclic peptidic competitive antagonists of uPA/uPAR-interaction such as WX-360 and WX-360-Nle have been developed which efficiently block binding of uPA to uPAR (Schmiedeberg *et al*., 2000, Magdolen *et al*., 2001, Guthaus *et al*., 2002). **(B)** Structures of WX-360 ($cyclo^{21,29}$[D-Cys21] -uPA_{21-30}[S21C;H29C]) and its norleucine derivative WX-360-Nle ($cyclo^{21,29}$[D-Cys21]-uPA_{21-30} [S21C;K23Nle;H29C]). The arrows point to the side chain of lysine (K^{23}) in WX-360 and norleucine (Nle^{23}) in WX-360-Nle, respectively.

After intraperitoneal inoculation of 3.0×10^7 *lacZ*-tagged OvMz-6-BAK cells, mice were treated once a day in a blinded manner, either with synthetic cyclic peptides (WX-360 or WX-360-Nle; 20 mg/kg/day) or vehicle until for 37 days. The mice were sacrificed, intraperitoneal organs are removed and stained with X-gal. To describe any therapeutic effect of the different peptides, tumor weight over total situs weight was assessed. In the control group, large tumor nodules on the left peritoneum and beneath the liver (near the site of tumor cell inoculation), as well as an abundant tumor spread across the peritoneal muscle layer, mesenterium, and the diaphragm was observed. By treating the mice with WX-360 and WX-360-Nle, fewer and smaller tumor nodules were present than in the control animals. Often (3 of 15 mice in both the WX-360- and WX-360-Nle-treated groups *versus* 1 of 16 mice in the control group), a larger nodular tumor mass was not even detectable (Fig. 9). The statistical analysis of the ratios of tumor weight over total situs weight proved that treatment of mice carrying human ovarian cancer cells with synthetic uPA-derived cyclic peptides resulted in a significant reduction of tumor burden (WX-360 *versus* control, $p = 0.0002$; WX-360-Nle *versus* control, $p = 0.023$) if compared to the untreated control group (Fig. 10A). A trend towards a lower tumor weight in the WX-360 group was observed. Treatment of the nude mice by either peptide did not result in serious side effects during the time of treatment. However, after one week, in some mice treated with WX-360-Nle an obvious excitability was seen. In addition to the tumor weight, we also measured organ weights of the mice to assess organotoxic side effects of the peptides. No significant differences were observed between the three groups (Fig. 10B), suggesting that treatment with the peptides did not affect organ growth of the mice.

The total protein levels of selected markers (uPA, PAI-1 and uPAR) in sampled tissues of sacrificed mice were investigated by specific human ELISAs. Although there was substantial reduction of tumor burden in treatment group, we did not find significant difference between treated mice and control mice with respect to these antigen levels (Table 2).

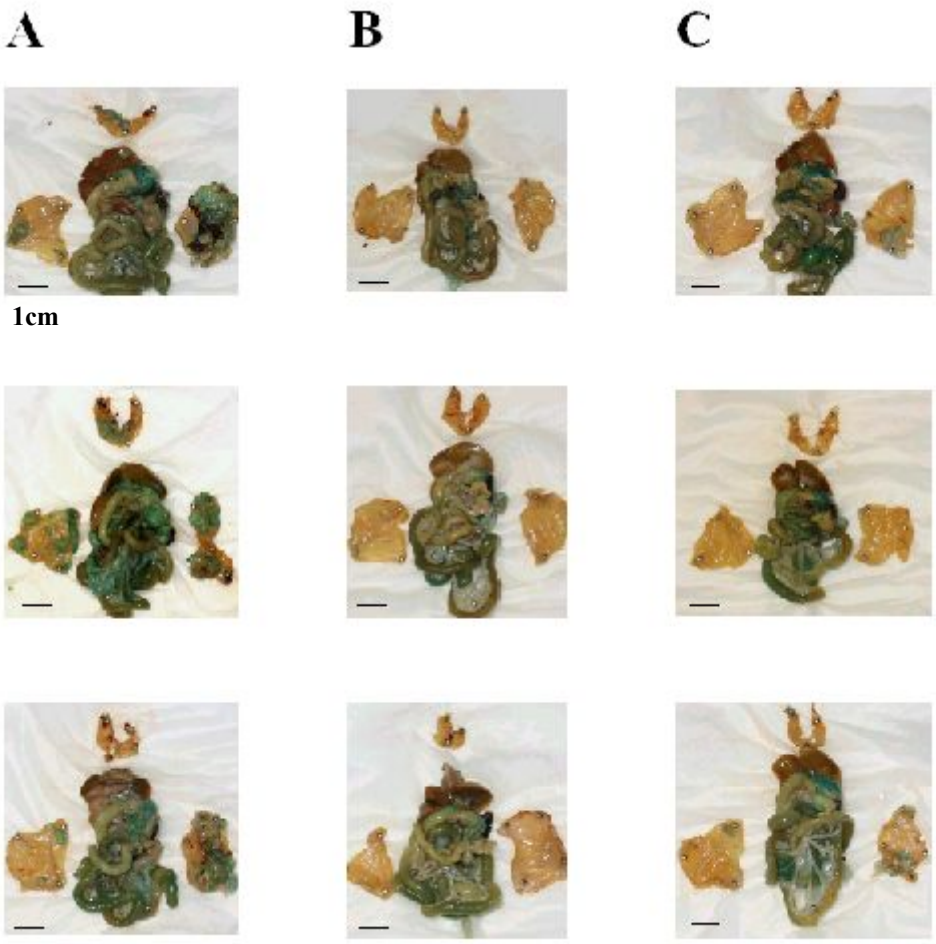

Figure 12. Tumor spread of OvMz-6-BAK cells within the peritoneum of the mouse: X-gal stained organs of mice treated with intraperitoneal injection of vehicle only (5 % mannitol, 0.6 % DMSO) **(A)**, WX-360 **(B)**, or WX-360-Nle **(C)** (37 days; treatment with 20 mg peptide/day/kg; a single injection per day). In the control group a large tumor nodule near the peritoneal inoculation site at the left side of the abdomen, as well as an abundant tumor spread across the peritoneal muscle layer, the mesenterium, and the diaphragm was observed at the end of the experiment **(A)**. In the groups of mice treated with the variant uPA-antagonists, fewer and smaller tumor nodules and strong reduction in tumor cell dissemination was observed **(B, C)**. Three representative examples of each group are depicted

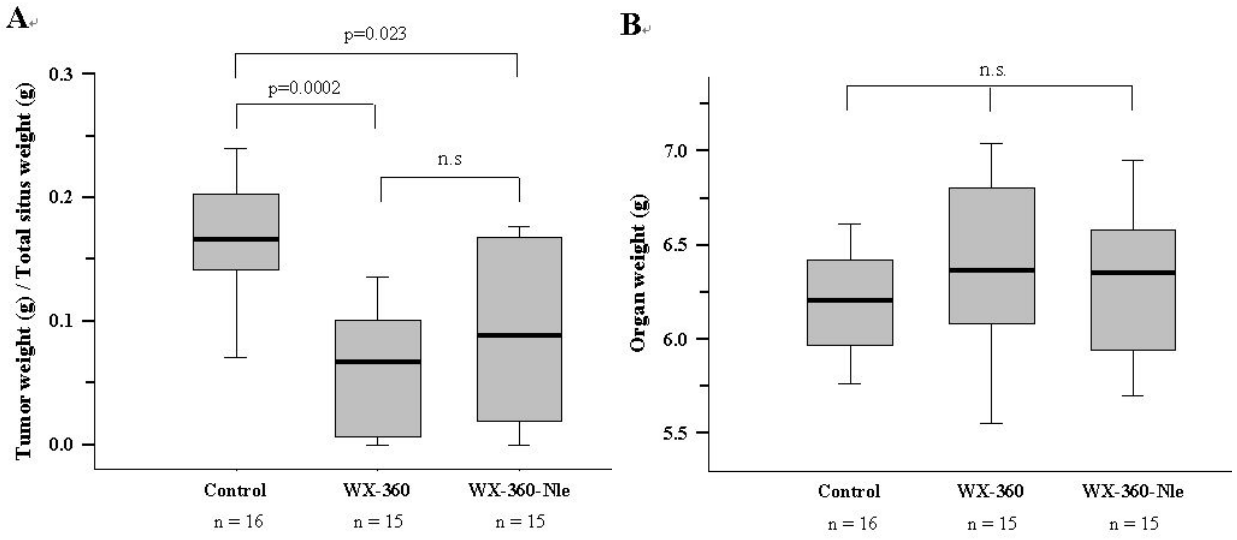

Figure 13. Effect of synthetic cyclic competitive uPA-derived peptide antagonists on primary tumor growth and spread: After inoculation of OvMz-6-BAK cells, nude mice were treated with either WX-360, WX-360-Nle (in each case 20 mg/kg/day), or vehicle for 37 days (single intraperitoneal injection per day). The groups were compared to each other with respect to tumor burden (given as the ratio of tumor weight over total situs weight) **(A)**, and organ weight **(B)**. The box plot indicates the 25th and 75th percentiles, the vertical bars mark the 10th and 90th percentiles, respectively. The median value is indicated by a bold bar. n.s., not significant.

	uPA	PAI-1	uPAR
	(ng/mg protein)	(ng/mg protein)	(ng/mg protein)
Tumor in treated mice [n=6]	12.9 ± 6.32	3.00 ± 1.12	1.58 ± 1.30
Tumor in control mice [n=4]	14.0 ± 4.81	2.83 ± 0.77	1.24 ± 0.44

Table 2. Antigen determination of uPA, uPAR and PAI-1 by ELISA. Antigen levels were determined in non-detergent cytosolic fractions of ovarian tumor tissue obtained from treated nude mice and control nude mice, using specific human ELISAs. All determinations were performed at least in duplicate and average number and standard deviation are given. The number in parenthesis indicates number of samples.

5. Discussion

The malignant features of a variety of solid tumors is associated with the pericellular uPA/uPAR system. In particular, the uPAR-mediated localization of active uPA to tumor cell surface receptor, uPAR, represents a crucial step for tumor cell proliferation, invasion, and metastasis, which is proved by the inhibitory action of a series of different therapeutic molecules targeted to uPA or uPAR at the protein or mRNA/gene level.

A considerable number of studies have already shown that interference with binding of uPA to its receptor uPAR leads to reduction of tumor invasion and metastasis. Therefore, this system with its increased activity in tumor cells represents an attractive target to attack tumor invasion and metastasis (Sperl *et al*., 2002). Several strategies for interfering with the uPA/uPAR interaction have been applied to date, including administration of antibodies to uPAR, synthetic peptides, and recombinant uPA-derived proteins as well as gene transfer of therapeutic molecules into tumor cells or host tissue by transfection with expression vectors or systemic adenoviral gene transfer.

One strategy to antagonize the uPA/uPAR system and to evaluate its role as a diagnostic and therapeutic target in metastatic cancer is the interruption of the uPA/uPAR interaction by specific blocking antibodies. Rabbani and Gladu generated a polyclonal antibody which is directed to the N-terminal uPA binding domain of rat uPAR (Rabbini and Glade 2002). The antimetastatic efficacy of this antibody was evaluated in a syngeneic model of rat breast cancer. For this, Mat B-III uPAR breast

cancer cells, which overexpress rat uPAR by stable transfection, were inoculated into the mammary fat pad of syngeneic female Fischer rats and the antibodies topically and daily applied for one week. Animals were dosed with anti r-uPAR antibodies from day 1-7 after tumor cell inoculation. These animals showed a marked decrease in tumor growth and a significant inhibition of metastasis to retroperitoneal and mesenteric lymph nodes as well as an obvious delay of metastasis to lung, liver, and spleen, respectively, when compared to control tumor-bearing animals receiving the same dose of preimmune rabbit IgG. Further analysis showed significantly increased tumor necrosis and cellular apoptosis (Rabbini and Glade 2002).

In order to specifically target uPAR-expressing cells, several approaches using fusion proteins have been undertaken in past years. Kobayashi and coworkers constructed a bifunctional hybrid molecule comprising aa 1-134 of uPA fused to the C-terminal domain II of the urinary trypsin inhibitor (UTI; aa 78-136), which efficiently inhibits plasmin. In an *in vivo* nude-mouse metastasis model, uPA1-134-UTI78-136 significantly reduced human ovarian carcinoma and choriocarcinoma cell spread to lungs and/or lymphatic tissues. Treatment with UTI domain II or ATF alone resulted in a relatively small therapeutic effect indicating a synergistic effect of both domains within the fusion protein (Kobayashi *et al*., 1998).

bi - trifunctional inhibitors encompassing functionally independent domains which are directed against the uPA/plasmin system, have been also successfully applied in *in vivo* models (Krol *et al*., 2003). A bifunctional inhibitor was generated by substitution of a loop within the cysteine protease inhibitor chicken cystatin with the uPA receptor (uPAR)-binding site of uPA (chCys-uPA$_{19-31}$; Muehlenweg *et al*., 2000). This

recombinant fusion protein inhibits both, the enzymatic activity of cysteine proteases and binding of uPA to its cell surface receptor uPAR, the latter representing a crucial step in activating the uPA/plasmin system. This concept was extended and trifunctional inhibitors that are also directed against matrix metalloproteinases (MMPs) were designed. It was demonstrated that these bi - trifunctional inhibitors inhibit cysteine proteases and MMPs while at the same time interfering with uPA/uPAR interaction by surface plasmon resonance technology. To test the impact of multifunctional inhibitors on tumor growth *in vi*vo, cell lines expressing these inhibitors were inoculated into the peritoneum of CD1 nude mice, resulting in a significant reduction of tumor burden and spread compared to a vector-transfected control cell line.

Another antagonistic fusion protein encompasses the uPAR binding GFD domain of either murine or human uPA (residues 1-48) and the constant region of human IgG. The engineered molecules exhibited potent, species specific binding affinity to uPAR accompanied by a marked improvement in pharmacokinetics compared to the GFD alone (Min *et al*., 1996, Tressler *et al*., 1999). Treatment of immunodeficient mice with these antagonists (s.c. application) significantly reduced primary tumor growth of human breast cancer cells (which had been subcutaneously injected into the mice). Both human and murine uPAR antagonists showed significant inhibition of primary tumor growth, demonstrating that *in vivo* tumor as well as stromal cells can contribute to uPAR dependent plasminogen activation or other uPAR activities, and by this, support tumor growth (Tressler *et al*., 1999). Moreover, the murine uPA based fusion protein substantially suppressed basic fibroblast growth factor-induced angiogenesis and B16 melanoma growth in syngeneic mice (Min *et al*., 1996).

Various transfection strategies targeting tumor cells or host tissue with cDNAs encoding components of the uPA system and variations thereof have been conducted in order to evaluate the potential of the uPA system as a target for cancer gene therapy. In an early study by Crowley and coworkers, a cDNA encoding a mutant uPA molecule, which lacks enzymatic activity due to replacement of the active site Ser356 by Ala but retaining uPAR binding affinity ([Ala356]uPA) was constructed. [Ala356]uPA was transfected into prostate cancer cells which were then inoculated into a spontaneous metastasis model (Crowly *et al*., 1993). When compared to parental cells, [Ala356]uPA-transfected cancer cells exhibited a significantly reduced metastatic potential to regional lymph nodes, brain, and lungs, respectively, whereas primary tumor growth was not affected by overexpression of [Ala356]uPA.

Exogenous addition of ATF reduced the *in vitro* invasiveness of uPAR-expressing cells derived from a primary carcinoma of the breast (Luparello *et al*., 1996). The same effect was noticed by overexpression of ATF in human lung giant-cell carcinoma cells (Zhu *et al*., 2001), and a recombinant adenovirus encoding murine ATF has been studied in a series of cancer models (Li *et al*., 1998). Liver metastasis was inhibited after intrasplenal inoculation of human LS174T colon carcinoma cells into nude mice after intranasal adenovirus delivery. Inhibition of primary tumor growth in nude mice was demonstrated by a single intratumoral injection of the ATF-encoding adenovirus into a pre-established MDA231 breast cancer subcutaneous tumor or into a pre-established syngeneic Lewis lung carcinoma. The reduction of tumor volume in both cases is thought to be due primarily to reduced angiogenesis since suppressed neovascularization within the tumor and in adjacent tissue close to the injection site of the tumor cells was observed, and the murine ATF expressed does not bind to human uPAR (Li *et al*., 1998).

Systemic adenoviral gene transfer of a chimeric protein composed of a mutant human ATF (mhATF) with high affinity for mouse and rat uPAR, linked to bovine pancreatic trypsin inhibitor (mhATF-BPTI) significantly inhibited subcutaneous tumor growth and decreased experimental lung metastasis in two rat bronchial carcinoma animal models (Zhu *et al*., 2001) and neointima formation and restenosis (Quax *et al*., 2001). In these tumor models, mhATF alone or human endostatin (even at ~ 10-fold higher molecular plasma concentrations than mhATF-BPTI or mhATF) did not lead to a significant inhibition of either tumor growth or metastasis (Legesvre *et al*., 2002).

In another experimental strategy, an expression plasmid encoding a soluble form of uPAR (suPAR) was transfected into human breast cancer cells (Krüger *et al*., 2000). Inoculation of those high level suPAR-expressing tumor cells resulted in significantly decreased experimental lung metastases when compared to parental tumor cells. While high expression levels of suPAR in breast cancer cells did not influence cell proliferation *in vitro*, tumor growth in the mammary fat pad of nude mice was markedly reduced (Krüger *et al*., 2000). However, in human ovarian cancer cells expressing high amounts of suPAR, a reduction of both cell proliferation *in vitro* and tumor burden (by up to 86 %) *in vivo* after intraperitoneal inoculation of these cells into nude mice was observed (Lutz *et al*., 2001), suggesting different roles for the uPAR system in tumor progression in different tissues.

All of these animal experiments provide "proof of principle" for the use of antagonists of uPA/uPAR-interaction in tumor inhibition. However, the application of large recombinant proteins for treatment of patients appears rather difficult and depends on sophisticated, *e.g.* viral, delivery systems (Sperl S. *et al*., 2002). Therefore, others and

we have concentrated on the development of small, synthetic competitive or non-competitive peptide antagonists (Bürgle *et al*., 1997, Goodson *et al*., 1994, Guo *et al*., 2000, Guthaus *et al*., 2002, Magdolen *et al*., 2001, Ploug *et al*., 2001, Schmiedeberg *et al*., 2002, Tressler *et al*., 1999).

A non-competitive peptide antagonist of the uPA/uPAR interaction derived from a non-receptor binding region of uPA (aa 136-143), Å6, reduced spontaneous metastasis of orthotopically growing human breast cancer cells in a mouse xenograft as well as tumor growth and spontaneous metastasis in a rat breast cancer model in syngeneic rats after intraperitoneal application (Guo *et al*., 2000, Guo *et al*., 2002). In the syngeneic rat breast cancer model the reduction of primary tumor growth by Å6 was further increased by combined treatment of Å6 with tamoxifen, a nonsteroidal antiestrogen (Guo *et al*., 2002). In a mouse xenograft model with human glioma cells, subcutaneous and intracranial tumor growth was inhibited upon daily application of Å6 (Mishima *et al*., 2000). Å6 inhibited breast cancer cell invasion but did not alter cell proliferation of these three tumor cell lines *in vitro*. Moreover, it led to decreased migration but not proliferation of human microvascular endothelial cells (Guo *et al*., 2000, Guo *et al*., 2002, Mishima *et al*., 2000). The anti-tumorigenic effect of Å6 is thus speculated to be at least in part a consequence of impaired tumor angiogenesis. Indeed, reduced tumor mass correlated with decreased microvessel density in all models. Å6 also increased apoptosis of human and rat cancer cells (Guo *et al*., 2002, Mishima *et al*., 2000). Despite these intriguing results the molecular basis of Å6 action is still poorly understood.

Several efforts have been undertaken over the years to develop competitive antagonists of uPA/uPAR-interaction that bind with high affinity to uPAR on tumor cell surfaces. One of the first approaches within this scenario was the use of synthetic peptides derived from the growth factor-like domain (GFD) of uPA (Kobayashi *et al*., 1994). Peptides of murine and human uPA were examined in order to determine whether they inhibit experimental and spontaneous lung metastasis by murine Lewis lung carcinoma cells. In an *in vivo* experimental metastasis assay, which determines mainly the later steps of the metastatic process, none of the peptides inhibited pulmonary metastases when co-injected intravenously into syngeneic mice. However, in an alternative *in vivo* test system that measures metastasis from a primary tumor (spontaneous metastasis model), multiple intraperitoneal injections of the murine uPA-derived peptide $muPA_{17-34}$ for one week after subcutaneous tumor cell inoculation, significantly blocked metastasis to the lung in a dose-dependent manner, whereas the human peptide uPA_{17-34} had no effect (Kobayashi *et al*., 1994).

Later, several linear peptides spanning uPA_{14-32} were synthesized in which the naturally occurring amino acids were individually replaced by alanine (Ala scan) in order to identify the amino acids critical for binding to uPAR (Magdolen *et al.,* 1996). The exchange of Cys19, Lys23, Tyr24, Phe25, Ile28, Trp30, and Cys31, respectively, by Ala resulted in peptides with strongly impaired uPAR-binding capacities, whereas replacement of the other amino acids had no or little effect on uPAR binding. Finally, the minimal uPAR-binding region of uPA was located to uPA_{19-31} using synthetic peptides which were successively shortened from the amino- and/or carboxy-terminus starting with uPA_{10-32} (Bürgle *et al.,* 1997). The region between amino acids Thr18 and Asn32 of uPA consists of a flexible, seven-residue Ω-loop (Asn22 to Ile28) which by

means of a double stranded, antiparallel ß-sheet (between Thr18 to Ser21 and His29 to Asn32) is forced into a ring-like structure (Hansen *et al*., 1994a, b; Magdolen *et al*., 1996; Schmitt *et al*., 2000). In uPA, Cys19 and Cys31, although in close proximity, form disulfide bonds with distinct cysteines (Cys11/Cys19 and Cys13/Cys31, respectively; Hansen *et al.,* 1994a, b). The short distance between Cys19 and Cys31 in the native molecule could lead cyclo^{19,31}uPA$_{19\text{-}31}$, which displays an even increased uPAR-binding activity (Bürgle *et al.,* 1997). Furthermore, systematic D-amino acid scan of uPA$_{19\text{-}31}$ are performed, in which each of the 13 L-amino acids was individually substituted by the corresponding D-amino acid. This led to the identification of cyclo^{19,31}[D-Cys19]-uPA$_{19\text{-}31}$ WX-307 as a potent inhibitor of uPA/uPAR-interaction, displaying only a 20 to 40-fold lower binding capacity as compared to the naturally occurring uPAR-ligands uPA and its amino-terminal fragment. These peptides not only block binding of uPA to uPAR but are also capable to displace uPAR-bound uPA from the cell surface and to inhibit uPA-mediated, tumor cell-associated plasminogen activation and fibrin degradation (Bürgle *et al*., 1997, Magdolen *et al*., 2001). cyclo^{19,31}-uPA$_{19\text{-}31}$ was evaluated in a pilot study in a xenogeneic mice tumor model with respect to its efficacy to suppress tumor growth and metastasis. Upon treatment of nude mice (n = 6) with a daily dose of 10 mg/kg, cyclo^{19,31}-uPA$_{19\text{-}31}$ reduced the growth of human MDA231 breast cancer cells after five weeks of treatment when compared to the vehicle-treated control group (Sperl *et al*., 2002).

Reduction of the ring-size and D-amino acid scanning led to WX-360 (cyclo^{21,29}[D-Cys21] uPA$_{21\text{-}30}$ [S21C;H29C]), displaying a 5-fold higher affinity towards uPAR than WX-307 (IC50: ~ 40 nM *versus* ~ 200 nM) (Guthaus E. *et al*., 2002, Schmiedeberg N. *et al*., 2000,). Furthermore, as WX-360 harbors a lysine

residue (K^{23}) and, thus, a target site for serine proteases such as plasmin, K^{23} was replaced by the non-protein amino acid norleucin (WX-360-Nle). This derivative still displays high binding affinity (IC50: ~ 70 nM). Stability-testing showed that both WX-360 and WX-360-Nle, respectively, were highly resistant to proteolytic degradation in human and rodent plasma or serum whereas other uPA-derived peptides lacking a non-natural D-amino acid (such as cyclo^{19,31}-uPA$_{16-32}$) were significantly less stable: after 1 hour incubation at 37 °C, peptide cyclo^{19,31}-uPA$_{16-32}$ was completely degraded, whereas WX-360 and WX-360-Nle, respectively, were stable over a period of 24 hours. After incubation with high amounts of plasmin (5 µg of peptide were incubated with 0.01 U [~ 4 µg] of plasmin at 37 ^{o}C), however, WX-360 was degraded, whereas WX-360-Nle was completely resistant to proteolysis (Schmiedeberg *et al.*, 2002).

In the present study, we demonstrate that treatment of with small, synthetic, cyclic, competitive uPAR-binding site-derived uPA antagonists results in a highly significant reduction of tumor burden and also dissemination in the peritoneal cavity *in vivo*. In the nude mouse model, we used OvMz-6 human ovarian cancer cells, which typically induce a large primary tumor and abundant intraperitoneal metastases (Lutz *et al.*, 2001). This cells showed fast proliferation, invasive characteristics and strong adhesion to ECM proteins in our *in vitro* analyses, which might explain the aggressive characteristics in the nude mice model.

The results of *in vivo* analysis are in line with those of a previous study, in which administration of Å6 synthetic non-competitive peptidic antagonist of uPA/uPAR interaction (75 mg per kg per day; two intraperitoneal injections per day), inhibited

tumor growth significantly, and suppressed the development of lymph node metastases in several breast cancer models (Guo *et al*., 2000).

Substitution of K^{23} in WX-360 with the non-protein amino acid norleucine did not significantly alter the biological efficacy of the peptide, although WX-360-Nle displays a further increased proteolytic stability as compared to its parent peptide WX-360. Compared to WX-360, WX-360-Nle is distinctly less soluble in aequeous solutions, because the exchange of the positively charged lysine side chain by the aliphatic norleucine side chain results in a zero net charge of the peptide. Interestingly, some mice developed an excitable behavior during the treatment with WX-360-Nle, which was characterized by heavy struggle against injections and an aggressive behavior beginning after the first week of administration. It is tempting to speculate that the lower solubility of WX-360-Nle may give rise to intraperitoneal peptidic precipitates. The behavioral changes in the mice receiving WX-360-Nle may be related to a poor tolerability of such intraperitoneal precipitates.

In conclusion, we have demonstrated that small synthetic cyclic competitive uPA peptide-antagonists can effectively reduce tumor growth and spread of human ovarian cancer cells in a mouse tumor model. These results strongly suggest that the peptides WX-360 and WX-360-Nle are sufficiently stable within the peritoneal cavity to efficiently interfere with uPA/uPAR-interaction on the tumor cells. Since ovarian cancer is a disease, which spreads throughout the abdominal cavity, putative new uPAR-directed drugs could be administered intraperitoneally. Thus, WX-360 and WX-360-Nle represent promising new compounds to inhibit tumor burden and dissemination of human ovarian carcinomas.

Malignant tumors are life-threatening because of its potential invade and abrogate the function of vital organs at distant sites, emphasizing the importance of targeting tumor metastasis to fight cancer. Since the interplay between several tumor proteolytic systems including plasminogen activation system facilitates extracellular matrix degradation, tumor invasion and metastasis, several synthetic inhibitors designed to attenuate the plasminogen activation system may eventually serve as novel therapeutic agents for cancer therapy in the near future.

6. Acknowledgements

I thank my supervisors, Dr. Viktor Magdolen, Prof. Dr. Manfred Schmitt (Klinische Forschergruppe der Frauenklinik), and Dr. Bernd Muehlenweg (Wilex AG) for helpful discussions and the opportunity to study a lot. I am also thankful to Prof. Dr. Hiroshi Kobayashi (Department of Obstetrics and Gynecology, Nara Medical University), Prof. Dr. Achim Krüger, Dr. Matthias Arlt, Dr. Charlotte Kopitz (Institut fur Experimentelle Onkologie und Therapieforschung), Sabine Creutzburg, Kawsar Bhuiyan, and Dr. Wolfgang Schmalix (Wilex AG) for their continuous and generous support of my work.

7. References

Andreasen, P. A., Egelund, R., and Petersen, H. H. The plasminogen activation system in tumor growth, invasion, and metastasis. Cell Mol.Life Sci., *57*: 25-40, 2000.

Appella, E., Robinson, E. A., Ullrich, S. J., Stoppelli, M. P., Corti, A., Cassani, G., and Blasi, F. The receptor-binding sequence of urokinase. A biological function for the growth-factor module of proteases. J.Biol.Chem., *262*: 4437-4440, 1987.

Brunner, N., Nielsen, H. J., Hamers, M., Christensen, I. J., Thorlacius-Ussing, O., and Stephens, R. W. The urokinase plasminogen activator receptor in blood from healthy individuals and patients with cancer. APMIS, *107*: 160-167, 1999.

Burgle, M., Koppitz, M., Riemer, C., Kessler, H., Konig, B., Weidle, U. H., Kellermann, J., Lottspeich, F., Graeff, H., Schmitt, M., Goretzki, L., Reuning, U., Wilhelm, O., and Magdolen, V. Inhibition of the interaction of urokinase-type plasminogen activator (uPA) with its receptor (uPAR) by synthetic peptides. Biol.Chem., *378*: 231-237, 1997.

Chapman, H. A., Riese, R. J., and Shi, G. P. Emerging roles for cysteine proteases in human biology. Annu.Rev.Physiol, *59*: 63-88, 1997.

Conese, M. and Blasi, F. Urokinase/urokinase receptor system: internalization/degradation of urokinase-serpin complexes: mechanism and regulation. Biol.Chem.Hoppe Seyler, *376*: 143-155, 1995.

Crowley, C. W., Cohen, R. L., Lucas, B. K., Liu, G., Shuman, M. A., and Levinson, A. D. Prevention of metastasis by inhibition of the urokinase receptor. Proc.Natl.Acad.Sci.U.S.A, *90*: 5021-5025, 1993.

Dano, K., Andreasen, P. A., Grondahl-Hansen, J., Kristensen, P., Nielsen, L. S., and Skriver, L. Plasminogen activators, tissue degradation, and cancer. Adv.Cancer Res., *44*: 139-266, 1985.

Del Rosso, M., Fibbi, G., Pucci, M., D'Alessio, S., Del Rosso, A., Magnelli, L., and Chiarugi, V. Multiple pathways of cell invasion are regulated by multiple families of serine proteases. Clin.Exp.Metastasis, *19*: 193-207, 2002.

Dublin, E., Hanby, A., Patel, N. K., Liebman, R., and Barnes, D. Immunohistochemical expression of uPA, uPAR, and PAI-1 in breast carcinoma. Fibroblastic expression has strong associations with tumor pathology. Am.J.Pathol., *157*: 1219-1227, 2000.

Duffy, M. J. Urokinase plasminogen activator and its inhibitor, PAI-1, as prognostic markers in breast cancer: from pilot to level 1 evidence studies. Clin.Chem., *48*: 1194-1197, 2002.

Duffy, M. J., Reilly, D., O'Grady, P., Collen, D., and Plow, E. F. Tissue-type and urokenase-type plasminogen activator as prognostic markers in breast cancer. In Fibrinolysis in disease Glass-Green-walt, CDC Press, New York, 14-18, 2001.

Ellis, V., Scully, M. F., and Kakkar, V. V. Plasminogen activation initiated by

single-chain urokinase-type plasminogen activator. Potentiation by U937 monocytes. J.Biol.Chem., *264*: 2185-2188, 1989.

Foekens, J. A., Buessecker, F., Peters, H. A., Krainick, U., van Putten, W. L., Look, M. P., Klijn, J. G., and Kramer, M. D. Plasminogen activator inhibitor-2: prognostic relevance in 1012 patients with primary breast cancer. Cancer Res., *55*: 1423-1427, 1995.

Fowler, B., Mackman, N., Parmer, R. J., and Miles, L. A. Binding of human single chain urokinase to Chinese Hamster Ovary cells and cloning of hamster u-PAR. Thromb.Haemost., *80*: 148-154, 1998.

Gardsvoll, H., Gilquin, B., Le Du, M. H., Menez, A., Jorgensen, T. J., and Ploug, M. Characterization of the functional epitope on the urokinase receptor. Complete alanine scanning mutagenesis supplemented by chemical cross-linking. J.Biol.Chem., *281*: 19260-19272, 2006.

Gardsvoll, H., Dano, K., and Ploug, M. Mapping part of the functional epitope for ligand binding on the receptor for urokinase-type plasminogen activator by site-directed mutagenesis. J.Biol.Chem., *274*: 37995-38003, 1999.

Goodson, R. J., Doyle, M. V., Kaufman, S. E., and Rosenberg, S. High-affinity urokinase receptor antagonists identified with bacteriophage peptide display. Proc.Natl.Acad.Sci.U.S.A, *91*: 7129-7133, 1994.

Grondahl-Hansen, J., Christensen, I. J., Rosenquist, C., Brunner, N., Mouridsen, H. T., Dano, K., and Blichert-Toft, M. High levels of urokinase-type plasminogen activator and its inhibitor PAI-1 in cytosolic extracts of breast carcinomas are associated with poor prognosis. Cancer Res., *53*: 2513-2521, 1993.

Guo, Y., Higazi, A. A., Arakelian, A., Sachais, B. S., Cines, D., Goldfarb, R. H., Jones, T. R., Kwaan, H., Mazar, A. P., and Rabbani, S. A. A peptide derived from the nonreceptor binding region of urokinase plasminogen activator (uPA) inhibits tumor progression and angiogenesis and induces tumor cell death in vivo. FASEB J., *14*: 1400-1410, 2000.

Guo, Y., Mazar, A. P., Lebrun, J. J., and Rabbani, S. A. An antiangiogenic urokinase-derived peptide combined with tamoxifen decreases tumor growth and metastasis in a syngeneic model of breast cancer. Cancer Res., *62*: 4678-4684, 2002.

Guthaus, E., Burgle, M., Schmiedeberg, N., Hocke, S., Eickler, A., Kramer, M. D., Sweep, C. G., Magdolen, V., Kessler, H., and Schmitt, M. uPA-silica-Particles (SP-uPA): a novel analytical system to investigate uPA-uPAR interaction and to test synthetic uPAR antagonists as potential cancer therapeutics. Biol.Chem., *383*: 207-216, 2002.

Hansen, A. P., Petros, A. M., Meadows, R. P., Nettesheim, D. G., Mazar, A. P., Olejniczak, E. T., Xu, R. X., Pederson, T. M., Henkin, J., and Fesik, S. W. Solution structure of the amino-terminal fragment of urokinase-type plasminogen activator. Biochemistry, *33*: 4847-4864, 1994.

Hansen, A. P., Petros, A. M., Meadows, R. P., and Fesik, S. W. Backbone dynamics of a two-domain protein: 15N relaxation studies of the amino-terminal fragment of urokinase-type plasminogen activator. Biochemistry, *33*: 15418-15424, 1994.

Harbeck, N., Kates, R. E., and Schmitt, M. Clinical relevance of invasion factors urokinase-type plasminogen activator and plasminogen activator inhibitor type 1 for individualized therapy decisions in primary breast cancer is greatest when used in combination. J.Clin.Oncol., *20*: 1000-1007, 2002.

Janicke, F., Prechtl, A., Thomssen, C., Harbeck, N., Meisner, C., Untch, M., Sweep, C. G., Selbmann, H. K., Graeff, H., and Schmitt, M. Randomized adjuvant chemotherapy trial in high-risk, lymph node-negative breast cancer patients identified by urokinase-type plasminogen activator and plasminogen activator inhibitor type 1. J.Natl.Cancer Inst., *93*: 913-920, 2001.

Kobayashi, H., Gotoh, J., Fujie, M., Shinohara, H., Moniwa, N., and Terao, T. Inhibition of metastasis of Lewis lung carcinoma by a synthetic peptide within growth factor-like domain of urokinase in the experimental and spontaneous metastasis model. Int.J.Cancer, *57*: 727-733, 1994.

Kobayashi, H., Sugino, D., She, M. Y., Ohi, H., Hirashima, Y., Shinohara, H., Fujie, M., Shibata, K., and Terao, T. A bifunctional hybrid molecule of the amino-terminal fragment of urokinase and domain II of bikunin efficiently inhibits tumor cell invasion and metastasis. Eur.J.Biochem., *253*: 817-826, 1998.

Kobayashi, H., Shinohara, H., Fujie, M., Gotoh, J., Itoh, M., Takeuchi, K., and Terao, T. Inhibition of metastasis of Lewis lung carcinoma by urinary trypsin inhibitor in experimental and spontaneous metastasis models. Int.J.Cancer, *63*: 455-462, 1995.

Kotzsch, M., Luther, T., Harbeck, N., Ockert, D., Lutz, V., Noack, F., Grossmann, D., Albrecht, S., Kramer, M. D., Lossnitzer, A., Grosser, M., Schmitt, M., and Magdolen, V. New ELISA for quantitation of human urokinase receptor (CD87) in cancer. Int.J.Oncol., *17*: 827-834, 2000.

Krol, J., Sato, S., Rettenberger, P., Assfalg-Machleidt, I., Schmitt, M., Magdolen, V., and Magdolen, U. Novel bi- and trifunctional inhibitors of tumor-associated proteolytic systems. Biol.Chem., *384*: 1085-1096, 2003.

Kruger, A., Soeltl, R., Lutz, V., Wilhelm, O. G., Magdolen, V., Rojo, E. E., Hantzopoulos, P. A., Graeff, H., Gansbacher, B., and Schmitt, M. Reduction of breast carcinoma tumor growth and lung colonization by overexpression of the soluble urokinase-type plasminogen activator receptor (CD87). Cancer Gene Ther., *7*: 292-299, 2000.

Kruger, A., Schirrmacher, V., and Khokha, R. The bacterial lacZ gene: an important tool for metastasis research and evaluation of new cancer therapies. Cancer Metastasis Rev., *17*: 285-294, 1998.

Lefesvre, P., Attema, J., and van Bekkum, D. Adenoviral gene transfer of angiostatic ATF-BPTI inhibits tumour growth. BMC.Cancer, *2*: 17, 2002.

Li, H., Lu, H., Griscelli, F., Opolon, P., Sun, L. Q., Ragot, T., Legrand, Y., Belin, D., Soria, J., Soria, C., Perricaudet, M., and Yeh, P. Adenovirus-mediated delivery of a uPA/uPAR antagonist suppresses angiogenesis-dependent tumor growth and dissemination in mice. Gene Ther., *5*: 1105-1113, 1998.

Llinas, P., Le Du, M. H., Gardsvoll, H., Dano, K., Ploug, M., Gilquin, B., Stura, E. A., and Menez, A. Crystal structure of the human urokinase plasminogen activator receptor bound to an antagonist peptide. EMBO J., *24*: 1655-1663, 2005.

Look, M. P., van Putten, W. L., Duffy, M. J., Harbeck, N., Christensen, I. J., Thomssen, C., Kates, R., Spyratos, F., Ferno, M., Eppenberger-Castori, S., Sweep, C. G., Ulm, K., Peyrat, J. P., Martin, P. M., Magdelenat, H., Brunner, N., Duggan, C., Lisboa, B. W., Bendahl, P. O., Quillien, V., Daver, A., Ricolleau, G., Meijer-van Gelder, M. E., Manders, P., Fiets, W. E., Blankenstein, M. A., Broet, P., Romain, S., Daxenbichler, G., Windbichler, G., Cufer, T., Borstnar, S., Kueng, W., Beex, L. V., Klijn, J. G., O'Higgins, N., Eppenberger, U., Janicke, F., Schmitt, M., and Foekens, J. A. Pooled analysis of prognostic impact of urokinase-type plasminogen activator and its inhibitor PAI-1 in 8377 breast cancer patients. J.Natl.Cancer Inst., *94*: 116-128, 2002.

Luparello, C. and Del Rosso, M. In vitro anti-proliferative and anti-invasive role of aminoterminal fragment of urokinase-type plasminogen activator on 8701-BC breast cancer cells. Eur.J.Cancer, *32A*: 702-707, 1996.

Lutz, V., Reuning, U., Kruger, A., Luther, T., von Steinburg, S. P., Graeff, H., Schmitt, M., Wilhelm, O. G., and Magdolen, V. High level synthesis of recombinant soluble

urokinase receptor (CD87) by ovarian cancer cells reduces intraperitoneal tumor growth and spread in nude mice. Biol.Chem., *382*: 789-798, 2001.

Magdolen, V., Burgle, M., de Prada, N. A., Schmiedeberg, N., Riemer, C., Schroeck, F., Kellermann, J., Degitz, K., Wilhelm, O. G., Schmitt, M., and Kessler, H. Cyclo19,31[D-Cys19]-uPA19-31 is a potent competitive antagonist of the interaction of urokinase-type plasminogen activator with its receptor (CD87). Biol.Chem., *382*: 1197-1205, 2001.

Magdolen, V., Rettenberger, P., Koppitz, M., Goretzki, L., Kessler, H., Weidle, U. H., Konig, B., Graeff, H., Schmitt, M., and Wilhelm, O. Systematic mutational analysis of the receptor-binding region of the human urokinase-type plasminogen activator. Eur.J.Biochem., *237*: 743-751, 1996.

Min, H. Y., Doyle, L. V., Vitt, C. R., Zandonella, C. L., Stratton-Thomas, J. R., Shuman, M. A., and Rosenberg, S. Urokinase receptor antagonists inhibit angiogenesis and primary tumor growth in syngeneic mice. Cancer Res., *56*: 2428-2433, 1996.

Mishima, K., Mazar, A. P., Gown, A., Skelly, M., Ji, X. D., Wang, X. D., Jones, T. R., Cavenee, W. K., and Huang, H. J. A peptide derived from the non-receptor-binding region of urokinase plasminogen activator inhibits glioblastoma growth and angiogenesis in vivo in combination with cisplatin. Proc.Natl.Acad.Sci.U.S.A, *97*: 8484-8489, 2000.

Mobus, V. J., Moll, R., Gerharz, C. D., Kieback, D. G., Weikel, W., Hoffmann, G., and

Kreienberg, R. Establishment of new ovarian and colon carcinoma cell lines: differentiation is only possible by cytokeratin analysis. Br.J.Cancer, *69*: 422-428, 1994.

Mondino, A., Resnati, M., and Blasi, F. Structure and function of the urokinase receptor. Thromb.Haemost., *82 Suppl 1*: 19-22, 1999.

Muehlenweg, B., Assfalg-Machleidt, I., Parrado, S. G., Burgle, M., Creutzburg, S., Schmitt, M., Auerswald, E. A., Machleidt, W., and Magdolen, V. A novel type of bifunctional inhibitor directed against proteolytic activity and receptor/ligand interaction. Cystatin with a urokinase receptor binding site. J.Biol.Chem., *275*: 33562-33566, 2000.

Muehlenweg, B., Sperl, S., Magdolen, V., Schmitt, M., and Harbeck, N. Interference with the urokinase plasminogen activator system: a promising therapy concept for solid tumours. Expert.Opin.Biol.Ther., *1*: 683-691, 2001.

Noel, A., Gilles, C., Bajou, K., Devy, L., Kebers, F., Lewalle, J. M., Maquoi, E., Munaut, C., Remacle, A., and Foidart, J. M. Emerging roles for proteinases in cancer. Invasion Metastasis, *17*: 221-239, 1997.

Novak, J. F. and Trnka, F. Proenzyme therapy of cancer. Anticancer Res., *25*: 1157-1177, 2005.

Ohkoshi, M. and Okuda, S. Growth inhibition of mouse autochthonous skin cancer by oral administration of new serine protease inhibitor ONO-3403. Anticancer Res., *22*:

821-823, 2002.

Pedersen, N., Schmitt, M., Ronne, E., Nicoletti, M. I., Hoyer-Hansen, G., Conese, M., Giavazzi, R., Dano, K., Kuhn, W., Janicke, F., and . A ligand-free, soluble urokinase receptor is present in the ascitic fluid from patients with ovarian cancer. J.Clin.Invest, *92*: 2160-2167, 1993.

Petersen, L. C., Lund, L. R., Nielsen, L. S., Dano, K., and Skriver, L. One-chain urokinase-type plasminogen activator from human sarcoma cells is a proenzyme with little or no intrinsic activity. J.Biol.Chem., *263*: 11189-11195, 1988.

Ploug, M., Gardsvoll, H., Jorgensen, T. J., Lonborg, H. L., and Dano, K. Structural analysis of the interaction between urokinase-type plasminogen activator and its receptor: a potential target for anti-invasive cancer therapy. Biochem.Soc.Trans., *30*: 177-183, 2002.

Ploug, M., Ostergaard, S., Gardsvoll, H., Kovalski, K., Holst-Hansen, C., Holm, A., Ossowski, L., and Dano, K. Peptide-derived antagonists of the urokinase receptor. affinity maturation by combinatorial chemistry, identification of functional epitopes, and inhibitory effect on cancer cell intravasation. Biochemistry, *40*: 12157-12168, 2001.

Ploug, M. Identification of specific sites involved in ligand binding by photoaffinity labeling of the receptor for the urokinase-type plasminogen activator. Residues located at equivalent positions in uPAR domains I and III participate in the assembly of a

composite ligand-binding site. Biochemistry, *37*: 16494-16505, 1998.

Ploug, M., Ronne, E., Behrendt, N., Jensen, A. L., Blasi, F., and Dano, K. Cellular receptor for urokinase plasminogen activator. Carboxyl-terminal processing and membrane anchoring by glycosyl-phosphatidylinositol. J.Biol.Chem., *266*: 1926-1933, 1991.

Quax, P. H., Lamfers, M. L., Lardenoye, J. H., Grimbergen, J. M., de Vries, M. R., Slomp, J., de Ruiter, M. C., Kockx, M. M., Verheijen, J. H., and van Hinsbergh, V. W. Adenoviral expression of a urokinase receptor-targeted protease inhibitor inhibits neointima formation in murine and human blood vessels. Circulation, *103*: 562-569, 2001.

Rabbani, S. A. and Gladu, J. Urokinase receptor antibody can reduce tumor volume and detect the presence of occult tumor metastases in vivo. Cancer Res., *62*: 2390-2397, 2002.

Rabbani, S. A., Harakidas, P., Davidson, D. J., Henkin, J., and Mazar, A. P. Prevention of prostate-cancer metastasis in vivo by a novel synthetic inhibitor of urokinase-type plasminogen activator (uPA). Int.J.Cancer, *63*: 840-845, 1995.

Reuning, U., Magdolen, V., Wilhelm, O., Fischer, K., Lutz, V., Graeff, H., and Schmitt, M. Multifunctional potential of the plasminogen activation system in tumor invasion and metastasis (review). Int.J.Oncol., *13*: 893-906, 1998.

Rijken, D. C. Plasminogen activators and plasminogen activator inhibitors: biochemical aspects. Baillieres Clin.Haematol., *8*: 291-312, 1995.

Schmiedeberg, N., Burgle, M., Wilhelm, O., Lottspeich, F., Graeff, H., Schmitt, M., Magdolen, V., and Kessler, H. in: Peptides for the New Millennium, Proceedings of the Sixteenth American Peptide Symposium (Fields, G.B., Tam, J.P. and Barany, G., Eds.). Kluwer Academic Publishers, Dordrecht., 543-545, 2000.

Schmiedeberg, N., Schmitt, M., Rolz, C., Truffault, V., Sukopp, M., Burgle, M., Wilhelm, O. G., Schmalix, W., Magdolen, V., and Kessler, H. Synthesis, solution structure, and biological evaluation of urokinase type plasminogen activator (uPA)-derived receptor binding domain mimetics. J.Med.Chem., *45*: 4984-4994, 2002.

Schmitt, M., Wilhelm, O., Reuning, U., Kruger A., Harbeck, N., Lengyel, E., Graeff, H., Gansbacher, B., Kssler, H., Burgle, M., Sturzebecher, J., Sperl, S., and Magdolen, V. The urokinase plasminogen activator system as a novel target for tumour therapy. Fibrinolysis and Proteolysis, *14*: 114-132, 2000.

Schmitt, M., Wilhelm, O., Janicke, F., Magdolen, V., Reuning, U., Ohi, H., Moniwa, N., Kobayashi, H., Weidle, U., and Graeff, H. Urokinase-type plasminogen activator (uPA) and its receptor (CD87): a new target in tumor invasion and metastasis. J.Obstet.Gynaecol., *21*: 151-165, 1995.

Schmitt, M., Harbeck, N., Thomssen, C., Wilhelm, O., Magdolen, V., Reuning, U., Ulm, K., Hofler, H., Janicke, F., and Graeff, H. Clinical impact of the plasminogen

activation system in tumor invasion and metastasis: prognostic relevance and target for therapy. Thromb.Haemost., *78*: 285-296, 1997.

Sier, C. F., Stephens, R., Bizik, J., Mariani, A., Bassan, M., Pedersen, N., Frigerio, L., Ferrari, A., Dano, K., Brunner, N., and Blasi, F. The level of urokinase-type plasminogen activator receptor is increased in serum of ovarian cancer patients. Cancer Res., *58*: 1843-1849, 1998.

Sperl, S., Muller, M., Wilhelm, O. G., Schitt, M., Magdolen, V., and Moroder, L. The uPA/uPAR System as a target for tumor therapy. Drug News Perspect, *14*: 401-411, 2002.

Tressler, R. J., Pitot, P. A., Stratton, J. R., Forrest, L. D., Zhuo, S., Drummond, R. J., Fong, S., Doyle, M. V., Doyle, L. V., Min, H. Y., and Rosenberg, S. Urokinase receptor antagonists: discovery and application to in vivo models of tumor growth. APMIS, *107*: 168-173, 1999.

Wermuth, J., Goodman, S. L., Jonczyk, A., and Kessler, H. Stereoisomerism and biological activity of the selective and superactive αvβ3 integrin inhibitor cyclo(-RGDfV-) and its retro-inverso peptide. J.Am.Chem.Soc., *119*: 1328-1335, 1997.

Wilhelm, O., Weidle, U., Hohl, S., Rettenberger, P., Schmitt, M., and Graeff, H. Recombinant soluble urokinase receptor as a scavenger for urokinase-type plasminogen activator (uPA). Inhibition of proliferation and invasion of human ovarian cancer cells. FEBS Lett., *337*: 131-134, 1994.

Wilhelm, O., Schmitt, M., Hohl, S., Senekowitsch, R., and Graeff, H. Antisense inhibition of urokinase reduces spread of human ovarian cancer in mice. Clin.Exp.Metastasis, *13*: 296-302, 1995.

Witschi, H. and Kennedy, A. R. Modulation of lung tumor development in mice with the soybean-derived Bowman-Birk protease inhibitor. Carcinogenesis, *10*: 2275-2277, 1989.

Yan, S., Sameni, M., and Sloane, B. F. Cathepsin B and human tumor progression. Biol.Chem., *379*: 113-123, 1998.

Zhu, F., Jia, S., Xing, G., Gao, L., Zhang, L., and He, F. cDNA transfection of amino-terminal fragment of urokinase efficiently inhibits cancer cell invasion and metastasis. DNA Cell Biol., *20*: 297-305, 2001.

Sumito Sato

Curriculum Vitae

Date of Birth	November 29, 1976
Place of Birth	Sapporo, Japan
Gender	Male
Nationality	Japanese
Marital status	Married, one child
Language	Japanese, English
Recent address	4-1-1 C-603 Nara Aoba-ku Yokohama
	227-0038 Kanagawa Japan
Phone	090-5875-5569 (++81)
E-mail	sumitosato@yahoo.com

Education:

1992-1995 Atsugi Public High School, Kanagawa, Japan

1995-2003 Hamamatsu University School of Medicine, Shizuoka, Japan

August 2000 - November 2001
Exchange student at the Clinical Research Unit at the Department of Obstetrics and Gynecology, Klinikum rechts der Isar, Technische Universität München, Germany

December 2001 - June 2002
Exchange student at the School of Biological and Molecular Sciences, Oxford Brookes University, UK

July 2002
Elective clerkship at the Shriners Hospitals for Children, Honolulu, USA

March 2003
Graduation at the Hamamatsu University School of Medicine, passed the national examinations to be awarded the Japanese degree of Doctor of Medicine (M.D.).

2003 - 2005
General Surgery Internship at Graduate School of Medicine, Chiba University Hospital, Chiba, Japan

2005 - 2006
Visiting scientist at the Clinical Research Unit at the Department of Obstetrics and Gynecology, Klinikum rechts der Isar, Technische Universität München, Munich, Germany

2007 - Present
General Surgery resident at Yokohama Asahi Hospital, Kanagawa, Japan